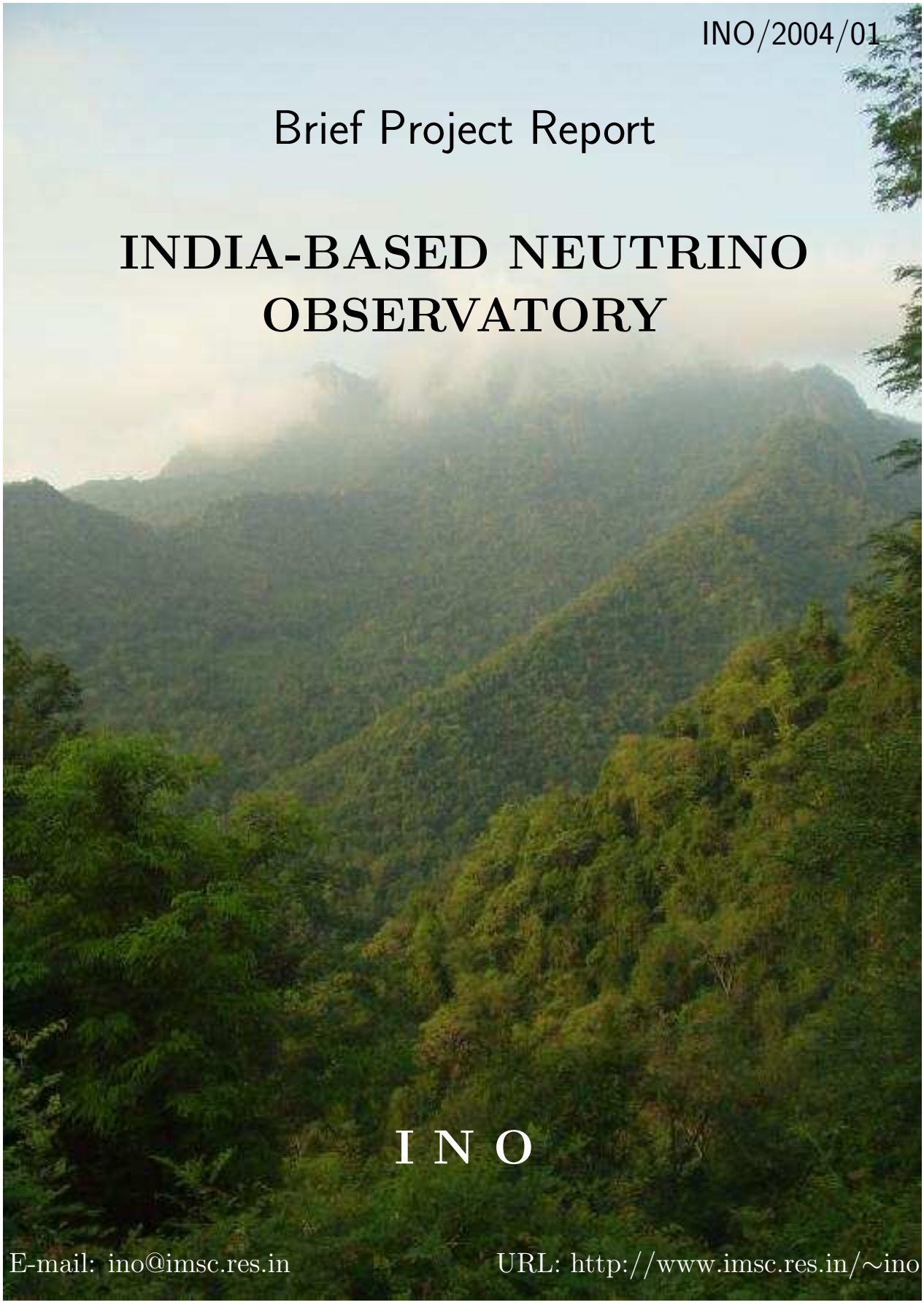

INO/2004/01

Brief Project Report

INDIA-BASED NEUTRINO OBSERVATORY

I N O

E-mail: ino@imsc.res.in URL: http://www.imsc.res.in/∼ino

PREFACE

Very important developments have occured recently in neutrino physics and neutrino astronomy. Oscillations of neutrinos and the inferred discovery that neutrinos have mass are likely to have far-reaching consequences. This discovery has come from the study of solar and cosmic ray produced neutrinos.

The pioneering solar neutrino experiments of Davis and collaborators in USA, the gigantic Super-Kamiokande detector in Japan and the heavy-water detector at the Sudbury Neutrino Observatory in Canada, and a few other laboratories, together, have contributed in a very fundamental way to our knowledge of neutrino properties and interactions. In particular, the Canadian experiment has given direct experimental proof of the 80-year-old thermonuclear hypothesis that the Sun and the stars are powered by thermonuclear fusion reactions.

Impelled by these discoveries and their implications for the future of particle physics, plans are being made now—world-wide—for new neutrino detectors, neutrino factories and long base-line neutrino experiments.

India was a pioneer in neutrino experiments. In fact cosmic ray produced neutrinos were first detected in the deep mines of Kolar Gold Fields (KGF) in 1965.

It is planned to revive underground neutrino experiments in India. A multi-institutional National Neutrino Collaboration has been formed with the objective of creating an India-based Neutrino Observatory (INO).

Feasibility studies for this project are in progress and an interim report based on these studies is nearing completion. What follows is a short report that summarises the main issues and questions that the collaboration would like to address. More details may be found on the INO web-site: http://www.imsc.res.in/∼ino.

Contents

Chapter 1

Introduction

Neutrino Physics is one of the fastest evolving fields in physics today. Neutrinos, introduced by Pauli in 1930, were first predicted to explain the continuous electron energy distribution in nuclear beta decay. Later they were christened as such by Fermi in 1934 who made them the basis for a theory of weak interactions. It was clear very early that these particles would be difficult to observe because their cross sections are so tiny. But in a series of experiments Reines and Cowan conclusively proved their existence through the inverse beta decay process, $\bar{\nu}_e + p \rightarrow e^+ + n$. Apart from electron-type neutrinos (which figure in nuclear beta decay), the separate identity of muon neutrinos was proved in 1962. The discovery of the τ lepton a decade later implied the existence of a third neutrino, ν_τ. It was only in the year 2001 that its existence was directly observed. A result of fundamental importance to neutrino physics is the precise measurement of the decay width of the Z-boson which is saturated by three active neutrino flavours.

In the "Standard Model"(SM) of particle physics, neutrinos are massless and come in three distinct flavours ν_e, ν_μ, ν_τ. In the SM there is no room for neutrino flavours to "oscillate" into other flavours. However, if the neutrino flavour states are mixtures of mass eigenstates with non-zero mass differences, then quantum mechanical evolution of these flavour states leads to the phenomenon of neutrino oscillations[1]. Experiments on solar neutrinos[2] and atmospheric neutrinos[3] have clearly indicated that neutrinos do exhibit such flavour oscillations and so at least two of them are indeed massive. This is the first indication for physics beyond the SM.

The sources of naturally occurring neutrinos are terrestrial and extraterrestrial. Furthermore, they are also produced in the laboratory. Each of these sources provides information, sometimes overlapping, that is extremely important in understanding the intrinsic properties of the neutrinos and their sources. The energy spectrum of naturally produced neutrinos starts from fractions of electron-volts and spans an impressive range. Fig. 1.1 shows the spectra of neutrinos from different sources as a function of their energies. Some of the spectra shown are based on observation while others, especially at high energies, are based on model calculations. While no single detector can fathom such a large range in energy, the very fact that neutrinos are produced over such a wide energy range poses challenging problems in their detection and understanding.

Neutrino physics has now come to occupy the centre stage of high energy physics, after the discovery of non-vanishing neutrino mass by observations of atmospheric neutrinos at the Super-Kamiokande underground laboratory in Japan as well as from observations of solar neutrinos at Super-Kamiokande[3] and the Sudbury Neutrino Observatory in Canada[2].

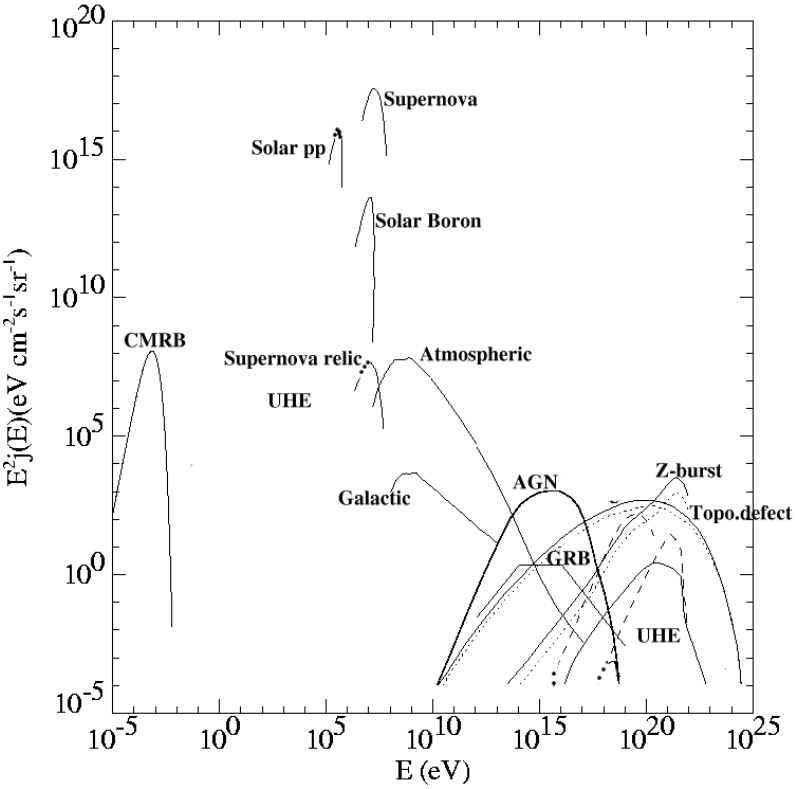

Figure 1.1: Neutrino spectra from different sources as a function of energy.[4]

This is the first evidence for physics beyond the standard model of particle physics. However, the estimated smallness of the neutrino mass (of the order of eV or much smaller) may have its origins near or beyond the scale of grand unified theories (GUTs), thus probing physics beyond the reach of present day accelerators.

1.1 Current Status

Experiments in the last several decades have provided many new and significant results. The main results may be summarised as follows:

- **Beta decay and double beta decay**: So far, there is only an upper limit on the mass of ν_e of 2.2 eV from Tritium beta decay. The limits on the other two states are much higher and not relevant in the light of present information on neutrino oscillations available. The neutrino-less double decay experiments which try to answer the question of whether the neutrino is a Majorana or Dirac particle (whether or not it is its own antiparticle) also suggest a mass of less than 0.2 eV if it were a Majorana particle. There is an upper limit on the sum of all the active neutrino masses, $\sum_i m_{\nu_i} < 0.7$ eV, from cosmological data. There are several experiments like KATRIN that are planned which will be capable of improving the limit to 0.3 eV. Future neutrino-less double beta decay experiments like GENIUS are capable of pushing the Majorana neutrino mass limit to 0.01 eV[5].

- **Solar and Atmospheric neutrinos**: The observation of the deficit in electron neutrinos from the Sun constitutes the Solar Neutrino Problem. The combination of deficit in charged current interactions (involving only electron neutrinos) and the lack thereof in neutral current interactions (involving all neutrino flavours identically) indicates that the solution to this problem is through neutrino oscillations. The best solution implies a mass squared difference of $\Delta m^2_{Solar} = 8.3 \times 10^{-5}$ eV^2 and large effects of solar matter in this oscillation process. The other anomaly involves the atmospheric muon neutrinos, whose deficit is accounted for by yet another mass squared difference $\Delta m^2_{Atm} = 2.2 \times 10^{-3}$ eV^2[6, 7]. These observations thus imply the existence of at least two non-zero masses for neutrino mass eigenstates.

- **Neutrinos from Supernova**: The observation of neutrinos from the Supernova SN1987a[8] has confirmed many qualitative features of the stellar collapse scenario. However, the number of observed events are statistically too small to draw conclusions on the properties of the neutrinos.

- **Other neutrino properties**: Stringent upper limits also exist for neutrino magnetic moments, life times, and other such properties. Future experiments like MUNU will improve the limit on the neutrino magnetic moment further[9].

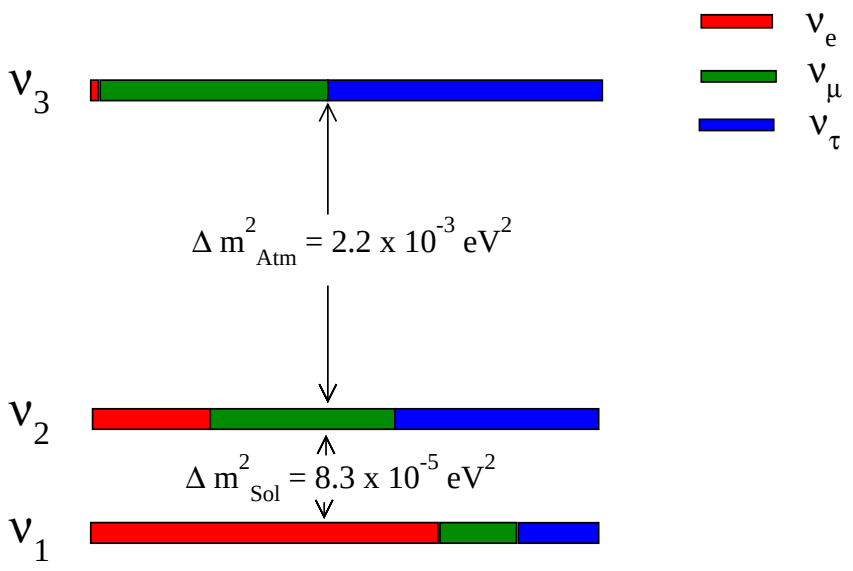

Figure 1.2: Schematic illustration of the status of masses and mixings of neutrino mass eigenstates. The extent of flavour states is indicated by different colours.

A summary of the present status of masses and mixings are shown in Fig.1.2 as obtained from a combined analysis of the pioneering experiments conducted at Homestake,

Sudbury, Kamioka, CHOOZ and KamLAND laboratories[1] This figure does not include the results obtained at LSND in Los Alamos laboratory[10], which are yet to be confirmed by an independent experiment.

In spite of these remarkable results, there are several outstanding issues of fundamental importance:

1. While there is definite evidence for the non-vanishing mass of neutrinos, the oscillation pattern itself over one full cycle, that is visible changes in the neutrino flux in terms of minima and maxima effect, has not been seen explicitly. However, the oscillation hypothesis remains a strong contender to explain various anomalies, especially after the recent results from Super Kamioka[11].

2. Analysis of solar and atmospheric neutrino data indicate that the mixing is dominantly between the (1–2) and the (2–3) sectors. The across-generation mixing, parametrised by the (1–3) mixing angle, θ_{13}, is known to be small , with $\sin^2 2\theta_{13} < 0.13$. However (modulo the LSND data), it is not known whether this angle is different from zero. It is the smallness of this angle that allows a separate two flavour analysis of both solar and atmospheric neutrino problems (see the next section for details).

3. What is the mass hierarchy of neutrinos? Assuming a three flavour scenario, it is only the solar neutrino mass squared difference whose sign is known, whereas the atmospheric neutrino data are so far insensitive to the sign of the mass squared difference between the participating neutrinos. This needs to be determined through the earth matter effects.

4. Is there CP violation in the leptonic sector? It is known that these effects are small; however, this is a question of fundamental and deep significance which may be probed in the future long-baseline neutrino experiments.

5. Do neutrinos decay? While this is unlikely as a dominant scenario to explain the known anomalies, it may still be allowed in combination with the neutrino oscillation, the latter being the dominant mechanism.

6. What is the absolute scale of neutrino mass? Direct mass measurements of the electron neutrinos puts an upper limit of about 2 eV. Interpretation of the recent results from WMAP[12] put the sum of the neutrino masses to around 0.7 eV. Neutrino-less double beta decay, if observed, will also determine the mass scale.

7. Are the neutrinos Dirac or Majorana particles? There is a strong theoretical prejudice that neutrinos are Majorana particles, but this can be established only by an unambiguous observation of neutrino-less double beta decay.

8. How many species of neutrinos exist? The number of active species with masses less than half the mass of the Z boson is limited to three by LEP experiments. However, results from the LSND experiment suggests the existence of at least one more, which has to be sterile, since there cannot be more than three light active species. Results from miniBOONE are awaited to confirm or rule out the LSND results.

[1]Note that we have chosen $m_3^2 - m_1^2 > 0$ in this figure. However, the present data does not distinguish between two possible hierarchies: $m_3^2 > m_2^2 > m_1^2$, $m_2^2 > m_1^2 > m_3^2$,

9. Does the neutrino have a non-zero magnetic moment? The existence of a magnetic moment for neutrino is of great fundamental importance (for example, μ_ν is possible only if the neutrino mass is nonzero). It will also have impact on the solar neutrino problem. Several experiments have already placed upper limits on $\mu_{\bar{\nu}}$ in the region $2 - 4 \times 10^{-10}\mu_B$ and this limit needs to be improved further..

Both at Sudbury and Kamioka the low energy solar neutrino experiments are still going on as also at Gran Sasso. Low energy reactor neutrino experiments are going on at laboratories such as KamLAND and CHOOZ. The low energy experiments are expected to give a near complete understanding of neutrino properties at this scale in not too distant a future. The atmospheric neutrino studies are expected to be augmented by those on GeV neutrinos produced and beamed from accelerators (or neutrino factories) at FNL, KEK and CERN. Some of the experiments being planned are at existing sites such as Gran Sasso, Kamiokande etc. In order to make measurements at several distances from the neutrino factories many Long Base Line stations are also being planned. One of these detectors, called MONOLITH[13], which was based on a 50 kton iron calorimeter, has the capability of unambiguously establishing the atmospheric neutrino oscillations as well as studying the neutrinos from CERN. There is need for such detectors. Some of the on-going and future detectors along with some of their important characteristics are mentioned in Table.1.1.

Experiment	Country	Type of detector	Major goals	Time schedule
Super-Kamiokande	Japan	Water Cerenkov	Solar, Supernova Atmospheric Long-baseline(K2K)	1996-
SNO	Canada	D_2O Cerenkov	Solar, Supernova	1999-
GNO	Italy	Gallium	Solar	1998-
ICARUS	Italy	Liquid Argon	Atmospheric Proton Decay Long-baseline	200?
KamLAND	Japan	Scintillator	Reactor	2001-
Double-CHOOZ	France	Scintillator	Reactor	2007
MiniBooNE	USA	Scintillator	Short baseline Fermilab booster	2003-
MINOS	USA	Iron Calorimeter	Long baseline Fermilab injector	2005
OPERA	Italy	Lead/Emulsion	Tau appearance	2005
MONOLITH	?	Iron Calorimeter	Atmospheric Long-baseline	?

Table 1.1: On-going and planned large scale neutrino experiments[14]

1.2 Genesis of INO

Historically the Indian initiatives in cosmic ray and neutrino physics go back to several decades. As a result of extensive studies of the muon flux at several depths in the Kolar

Gold mines, it was realised that the muon flux was low enough to permit measurements on atmospheric neutrinos. The first ever such neutrino interaction was observed as early as in 1965. Thus it is correct to say that the Kolar experiments were the harbingers of the present day atmospheric neutrino experiments[15]. This laboratory later looked for nucleon decay and placed upper limit on the half-life for the proton decay[16]. Another interesting finding is the observation of the so-called Kolar events, which have not been explained to date[17]. These suggested a decaying heavy particle with an amazingly long lifetime of a few nanosececonds. Most of these experiments were done using calorimeters weighing up to 300 tons in iron, with visual detectors (such as neon flash tubes) and proportional counters. Unfortunately the mines were closed down in 1990 and these experiments were discontinued. In view of the importance of the neutrino physics as outlined above and the past Indian contribution, it is felt that the Indian efforts in neutrino physics be revived.

Considering the physics possibilities and the past Indian experience, it was decided, after a prolonged discussion, to start with a modern iron calorimeter with Resistive Plate Chambers(RPC) as the active detector elements. The detector, to be described in the next section has to be housed in low background surroundings at a suitable place. The entire detector module is similar in design scale and capabilities to the MONOLITH detector[13] which was proposed at Gran Sasso and vetted by experts. However it is unlikely to be located at Gran Sasso due to space constraints and there are new proposals to install it at the proposed National Underground Science and Engineering Laboratory[18] at Homestake mines in USA.

Thus there is wide interest in this type of detector and a quick implementation of such a project can achieve many physics goals like:

- Unambiguous and more precise determination of **oscillation parameters** using atmospheric neutrinos.
- Study of **matter effects** through charge identification, that may lead to the determination of the unknown sign of one of the mass differences.
- End detector for a future **Long-baseline neutrino oscillation** experiment.
- **CPT violation** studies.
- **Kolar events**, possible identification of **Ultra-High energy** neutrinos and **multi-muon** events.

Although the INO will start its activity with the Iron Calorimeter(ICAL), it is envisaged that INO will ultimately have other neutrino experiments as well under its umbrella.

The geographical location for any India-based neutrino laboratory is particularly interesting, as most of the neutrino detectors are scattered around the world at latitudes above 35^o. There is none close to the equator as yet. It is possible to push such a detector down to almost 8^o latitude in South India. Such a location permits neutrino astronomy searches covering the whole celestial sky, study of solar neutrinos passing through the Earth's core and finally neutrino tomography of the Earth at a future date using terrestrial and laboratory neutrino sources.

After a survey of several possible sites in the country we discuss three most suitable sites, namely Singara in Nilgiris, Rammam in Darjeeling Himalayas and the proposed tunnel under the Rohtang Pass in Himachal Pradesh. We discuss this in a separate section.

This brief report concludes with a discussion of the general issues pertaining to an underground laboratory. We give a list of relevant reviews and websites at the end from which more information on the neutrino experiments and theory may be obtained.

INO[19] has been conceived on a scale that no other basic sciences project in India has attempted. It is a result of the enthusiasm shown by the neutrino physics community in India. The interest shown by international community in this project is also encouraging. Over time INO is expected to develop into a full fledged underground science laboratory to host experiments that require low background environment. The Laboratory may also host experiments in other disciplines such as geology and biology, that can profit from it special environment and infrastructure.

Chapter 2

The Detector

Once it was decided to concentrate on the atmospheric and long baseline neutrino physics, two basic detector types were discussed by the INO group. They are the **water Cerenkov detector**, similar to the existing Super-Kamiokande detector in Japan, and a **magnetised iron calorimeter**, which would be an extension of and improvement over the old KGF detector[16] and similar in design to the proposed MONOLITH[13] detector.

Since Super-K, with a 50 kton volume already exists, in order to compete internationally, or even to resolve some of the issues thrown up by Super-K, it will be necessary to go in for a very large water detector, of the order of one Megaton. The active detector elements, photo-multiplier tubes, required for this need to be developed in this country. Otherwise, this type of detector design is well-known and quite straightforward.

On the other hand, the magnetised iron calorimeter design is still in the R&D stage. The MONOLITH collaboration has proposed one such design for which approval while still pending is unlikely due to space constraints in Gran Sasso. The most exciting thing about this detector is that the magnetic field, in addition to improving range and resolution of energy, will be able to separate different charged particles, for example, it will distinguish μ^+ from μ^-. This is very crucial not only for CP violation studies but also to study earth matter effects on atmospheric neutrinos as well as being an absolute necessity for the far-end detector of a long base-line experiment such as is feasible at INO with the neutrino beam from a neutrino factory, in Japan or elsewhere.

2.1 ICAL: A Magnetised Iron Calorimeter with fast timing

Within the framework of atmospheric neutrino oscillation, the survival probability for ν_μ neutrinos in the two-flavour scheme is[1] (see the next chapter for more details)

$$P_{\mu\mu} = 1 - \sin^2 2\theta \sin^2(\frac{1.27\delta L}{E}) \ , \tag{2.1}$$

where L is the distance travelled in km, E is the energy of the neutrino in GeV, θ is the neutrino mixing angle and δ is the difference of the neutrino mass squared eigenvalues expressed in eV^2. Thus the survival probability is a simple oscillating function of L/E. A verification

[1] In principle the propagation of neutrinos involves all the three active flavours. Further, the matter effects also play an important role. To keep the arguments simple, we will not discuss these detailed issues here.

of the oscillation hypothesis requires an identification of the minima and maxima. The most recent analysis of Super-K events show evidence for the first dip and rise in $P_{\mu\mu}$. Although this measurement is very suggestive of muon neutrino oscillation, only an observation of the full oscillation pattern as a function of L/E over more than one period will constitute a confirmation of the oscillation scenario. This requires a detector which extends over a larger range of L/E with better E and L resolution (which requires an accurate measurement of the position and direction). These goals can be achieved by a good tracking calorimeter.

In such a detector the energy of the neutrinos could be measured very accurately by detecting the fully and partially confined events with the vertex inside the detector. Energy of fully confined events could be measured by track length methods whereas for partially confined events, the energy of the escaping muon could be well estimated from the bending of such a track in the magnetic field within the detector. The path length L, from the production point, covered by the neutrino could be estimated from the neutrino direction. A sub-nano-second time resolution, which ensures an almost perfect up-down discrimination of the event, is necessary for this. The L/E resolution is expected to improve with energy due to improved measurement of the direction of the higher energy muon. Thus a detector with a large mass (and high density) with good timing characteristics and with a magnetic field satisfies the requirement for such measurements.

2.1.1 Detector Structure

The proposed detector, see Fig. 2.1, will have two modules of lateral sizes 16 m $\times$ 16 m each and a height of about 12 m. This is composed of 140 layers of iron plates of thickness 6cm each,[2] inter-leavened with active detector elements of thickness 2.5cm each, to be described in the next subsection. The iron plates can be magnetised up to 1–1.4 Tesla. The total mass of such a detector including the support structure etc, will be approximately 35 kton. The plates can, in principle, be arranged horizontally or vertically depending on whether one is more interested in near vertical or horizontal neutrinos. The whole detector as described above is to be surrounded by an external layer of scintillation counters. This will act as a veto layer and will be used to identify muons entering the detector from outside as well as to identify partially confined events with vertex inside the detector. In addition to the main detector, two smaller detectors of equal area but with fewer layers of active detector elements is proposed to be located on either side of the main detector to increase the aperture to study neutrinos from astrophysical objects at a later stage.

2.1.2 Active Detector Elements

The total active area of the detector is $32 \times 16\ m^2$ between two successive planes, or a total 70000 square meters for the whole detector. Glass Spark Chambers (GSC) which are low cost active detectors[20] with nano-second timing resolution are well suited to span such a large area. The GSC, shown in Fig.2.2, is a gas filled detector (mixture of Argon, Freon and Iso-butane) with two parallel electrodes of 2mm thick float glass, having a volume resistivity of 10^{12}ohm-cm. The plates, kept 2mm apart by suitable spacers, contain the gas. For a suitable combination of gas mixture and electrical field the detector can be operated in a spark mode. The high resistivity of the electrodes and the choice of the gas mixture ensure the containment of the spark as well as the recovery time. The high voltage (in the range

[2]while this has been assumed throughout, it might change to 6.3cm which is the manufacturing standard.

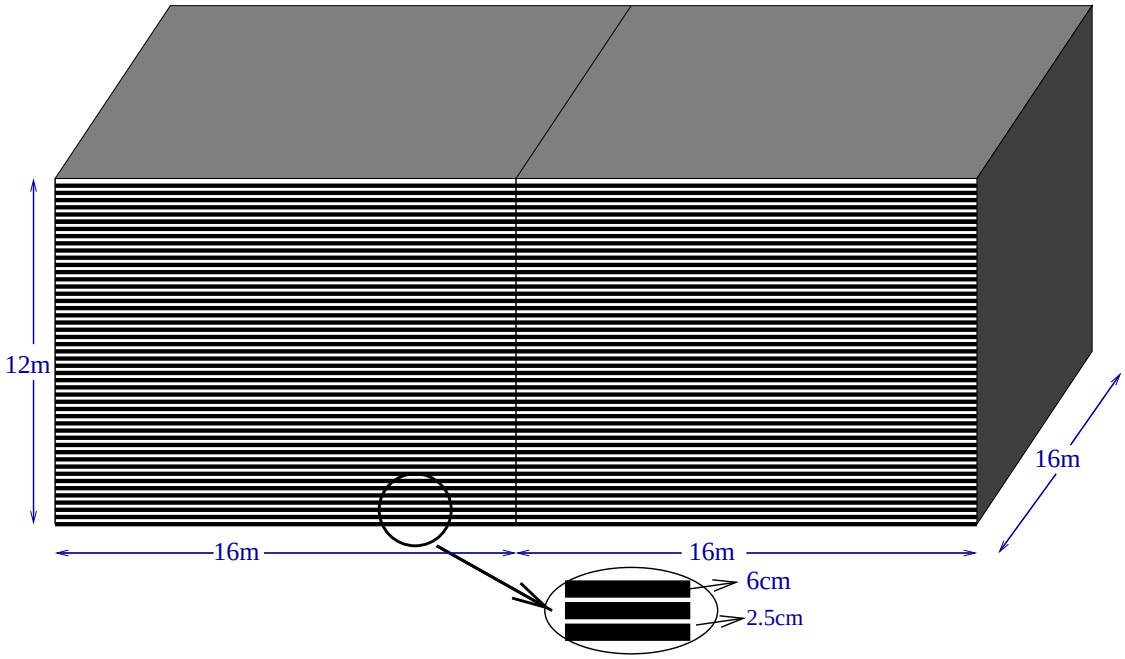

Figure 2.1: Sketch of the iron calorimeter detector.

of 8–10kV) will be applied to the electrodes either by means of graphite coating or resistive adhesive film on the glass plate.

A basic RPC detector element will be of 2m length and 2m wide. Eight such RPC elements will cover a road of 16m X 2m and will be read out by 64 pickup strips along the X direction (2m wide road) and 512 strips along the Y direction (16 m). There are a total of 16 roads in a layer, see Fig. 2.3. A total of around 18000 RPC detector elements will be required to complete the detector. The strip pickup planes will be realised either by gluing a grooved copper foil on one side of a plastic honey-comb the other side of which will have a continuous foil and will be grounded or by using a copper clad G10 sheet with readout strips grooved on one side and the other side acting as the ground plane. The spacial accuracy of about 1.5cm on both views can be obtained with such a read out.

The thickness of the detector tray to be inserted between two iron plates is about 2cm. The total number of GSC units will be about 18000. Thus the detector fabrication is a gigantic task due to the scale and requires active participation from industry.

2.2 Present Status

Prototype RPCs have been built at TIFR and SINP. An advanced gas mixing unit is designed at SINP with many built-in features for gas mixing. A major milestone has been crossed with the efficiency crossing 90% above 8.6 kV. In Fig.2.4 the performance of the prototype at TIFR is shown. Apart from the efficiency, the other important feature of this detector element is the fast timing which is useful for discriminating the up-going muons from the down-going muons. Furthermore, as shown in Fig.2.5, the timing is better or as good as in the case of a scintillator detector.

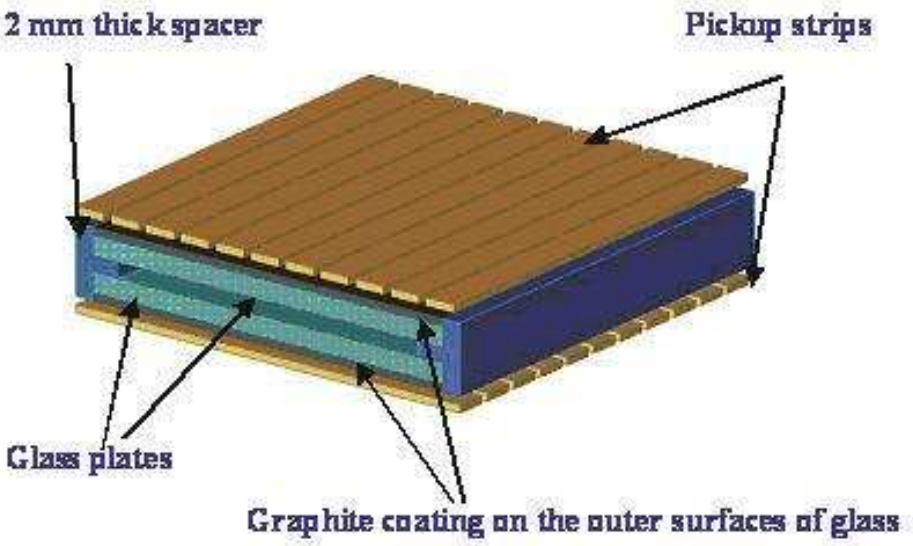

Figure 2.2: Sketch of a typical glass spark chamber.

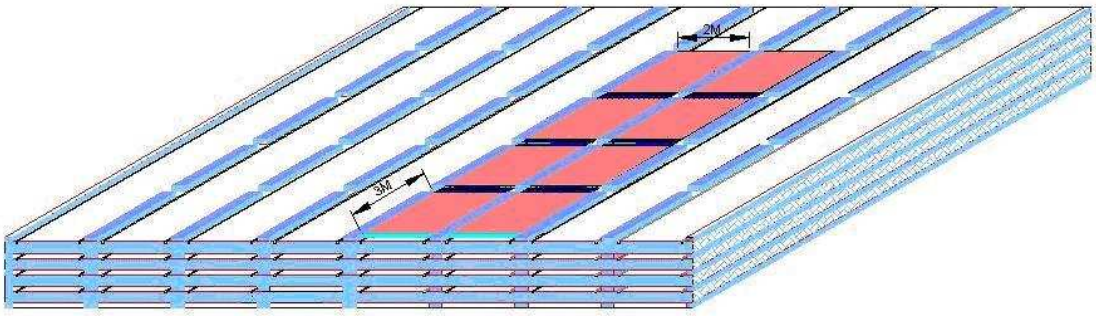

Figure 2.3: Basic detector elements: strip planes.

The detector R & D is now focussing on the following issues:

- RPC timing, charge distribution, noise and cross-talk.
- Mean Charge vs Voltage which appears to be linear.
- Gas composition and mixing. At present three gas mixture is being used with the concentration of isobutane kept at 8%. The content of Freon 134 and Argon are varied as shown in the figures Figs. 2.4 and 2.5.

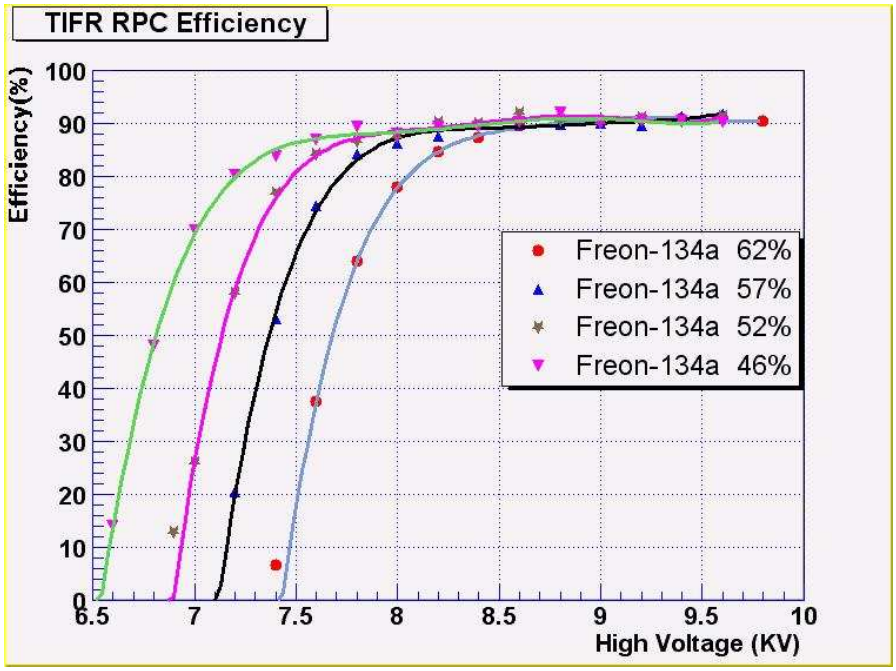

Figure 2.4: RPC efficiency as a function of HV for different gas compositions.

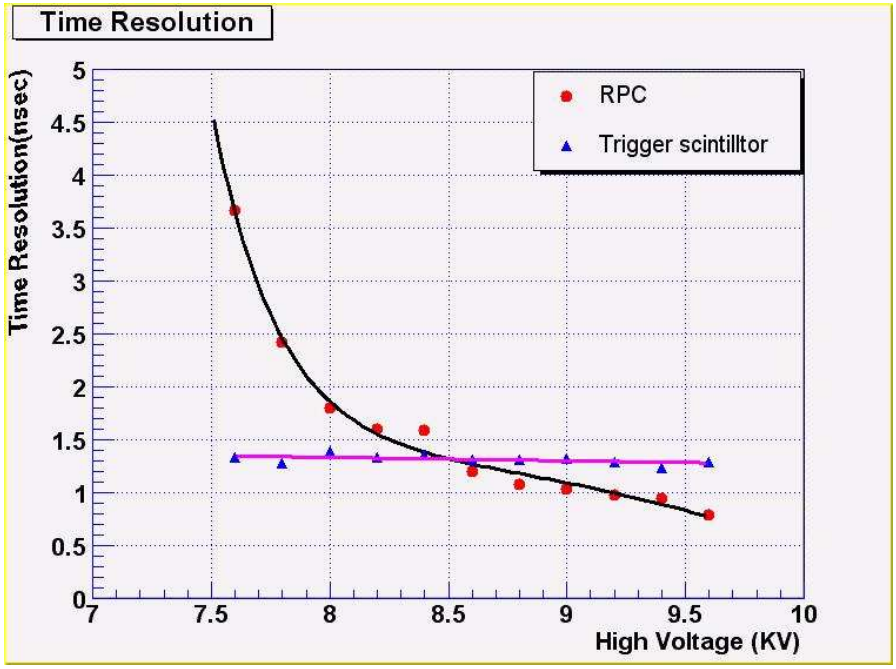

Figure 2.5: Comparison of the time resolution of the RPC and Scintillator.

To summarise, the main characteristic of the **ICAL** detector is a clean identification of muons with good energy and time resolution. Also, the presence of the magnetic field will distinguish positive and negative charged particles.

The design for magnetisation of ICAL is still at a very preliminary stage. The necessary software has been installed and the field mapping is in progress at BARC and VECC.

Chapter 3

Physics Issues

It is fair to say that over the last few years there has been a paradigm shift in the nature of the goals to be pursued in neutrino physics. From a search for understanding the particle physics and/or the astrophysics driving the solar and atmospheric neutrino deficits the focus has shifted to one where we seek to make increasingly *precise measurements of neutrino mass and mixing matrix parameters*. Experiments planned to yield results over the next fifteen to twenty years thus reflect this change in focus.

Almost all of the planned projects are long baseline [1] endeavours using:

1. *a conventional proton beam* colliding with a target to produce pions which then decay to give muon neutrinos,
2. *super-beams*, which are essentially technologically upgraded versions of present conventional beams, or,
3. *reactor sources* with both near and far detectors for reduced systematic errors,
4. *muon storage rings*, which exploit muon decay to produce intense and collimated neutrino beams.

Besides providing compelling evidence for non-zero neutrino mass and oscillations, along with ranges of possible mass and mixing parameters, they have, importantly, identified the experimental goals and directions the neutrino community must pursue over the next two decades. At this juncture the main goals of neutrino physics research are :

- Improve the precision of masses and mixing angles, that we already know.
- Determine the sign of the mass-squared difference (δ_{32}) involved in the atmospheric neutrino oscillations.
- Improve the existing upper limit on the mixing angle θ_{13} and to ascertain if its value is different from zero or not.
- Determine whether the leptonic CP phase δ is non-zero, and if so, obtain some measure of its magnitude.

[1] By "long baseline" we actually mean the L/E range of about 50-500 km/GeV. For accelerator experiments, this translates to baselines conventionally termed "long", but for the lower reactor neutrino energies, the baselines are actually 1-2 km.

- To substantiate/verify the observed oscillation dip by SK collaboration and conclusively show that oscillations are responsible for observed flux deficits by demonstrating an L/E dependence of event rates.
- Existence of sterile neutrinos.
- To determine whether neutrinos are Dirac and Majorana particles.
- Last but not the least, to probe any non-standard mechanism beyond neutrino oscillation due to mass and mixing occurring at a sub leading level.

Over the next 2 decades, the present and next generation experiments are likely to give us useful information on the goals mentioned above, and if we are lucky and θ_{13} is large, some very preliminary data relevant to this parameter. Different experimental facilities are being planned to improve the current bound on the solar and atmospheric parameters as well as to improve the sensitivity to θ_{13}, the CP violating phase δ and the sign of δ_{32}.

To summarise, planned experiments will, over the next 15-20 years, greatly improve the precision on δ_{31}, effect a very modest improvement in the existing measurements for $\sin^2\theta_{23}$, and improve the upper bound on $\sin^2\theta_{13}$ by a factor of two to six, depending on the experiment. We note that these experiments, given their insensitivity to matter effects, will not be able to determine the sign of δ_{31} and thus establish whether neutrino masses follow a normal hierarchy or an inverted one. They will thus leave one of the major questions of neutrino physics unaddressed.

We will see in the following how the above challenges can be addressed in the a setup like large magnetised iron calorimeter (ICAL) at INO, including the major open problem–**the sign of** δ_{31} even with atmospheric neutrinos. Below we first briefly describe the prospects of ICAL detector for atmospheric neutrinos and subsequently using it as an end detector of a high energy high intensity neutrino beam from a distant source. In order to understand the notations and concepts used in the text we give a brief introduction to the three-flavour-oscillation physics.

3.1 Three flavour oscillation

The neutrino flavour states $|\nu_\alpha\rangle(\alpha = e, \mu, \tau)$ are linear superpositions of the neutrino mass eigenstates $|\nu_i\rangle(i = 1, 2, 3)$ with masses m_i :

$$|\nu_\alpha\rangle = \sum_i U_{\alpha i}|\nu_i\rangle.$$

Here U is the 3×3 unitary matrix which may be parametrised as (ignoring Majorana phases)[21]:

$$U = \begin{pmatrix} c_{12}c_{13} & s_{12}c_{13} & s_{13}e^{-i\delta} \\ -c_{23}s_{12} - s_{23}s_{13}c_{12}e^{i\delta} & c_{23}c_{12} - s_{23}s_{13}s_{12}e^{i\delta} & s_{23}c_{13} \\ s_{23}s_{12} - c_{23}s_{13}c_{12}e^{i\delta} & -s_{23}c_{12} - c_{23}s_{13}s_{12}e^{i\delta} & c_{23}c_{13} \end{pmatrix}.$$

where $c_{12} = \cos\theta_{12}$, $s_{12} = \sin\theta_{12}$ etc., and δ denotes the CP violating (Dirac) phase. By definition, the 3×3 neutrino mass matrix M_ν is diagonalised by U:

$$U^\dagger M_\nu U = \mathrm{diag}(m_1, m_2, m_3). \tag{3.1}$$

The general expression for the probability that an initial ν_α of energy E gets converted to a ν_β after travelling a distance L in vacuum is

$$P_{\nu_\alpha\nu_\beta} = \delta_{\alpha\beta} - 4\sum_{i>j}\mathrm{Re}[U_{\alpha i}U^*_{\beta i}U^*_{\alpha j}U_{\beta j}]\sin^2\left(\frac{\pi L}{\lambda_{ij}}\right) + 2\sum_{i>j}\mathrm{Im}[U_{\alpha i}U^*_{\beta i}U^*_{\alpha j}U_{\beta j}]\sin\left(2\frac{\pi L}{\lambda_{ij}}\right),$$

where, $\lambda_{ij} = 2.47\mathrm{km}(E/\mathrm{GeV})(\mathrm{eV}^2/\delta_{ij})$, $\delta_{ij} = {m_j}^2 - {m_i}^2$. The above expression is given for vacuum. In matter, the probabilities are drastically modified.

3.2 Parameter values gleaned from experiments so far

We give the best-fit and allowed ranges of the parameters that appear in the 2 generation case.

- Allowed region from Solar + KamLAND Results : Assuming CPT invariance, the 3σ allowed range of parameters and the spread (in parenthesis) of δ_{21} and $\sin^2\theta_{12}$ from solar and recent 766.3 day KamLAND data[6] are given by

$$7.2\times10^{-5} < \delta_{21} \equiv \delta_{\mathrm{sol}} < 9.5\times10^{-5}\mathrm{eV}^2(14\%)$$
$$0.21 < \sin^2\theta_{12} \equiv \sin^2\theta_{\mathrm{sol}} < 0.37(27\%)$$

  The best-fit points are :$\delta_{21} = 8.3\times10^{-5}\mathrm{eV}^2$ and $\sin^2\theta_{12} = 0.27$.

- Atmospheric + K2K experiments : The allowed range at 3σ of parameters from atmospheric and K2K data[22] is

$$1.4\times10^{-3} < |\delta_{32}| \equiv \delta_{\mathrm{atm}} < 3.3\times10^{-3}\mathrm{eV}^2$$
$$0.34 \le \sin^2\theta_{23} \equiv \sin^2\theta_{\mathrm{atm}} \le 0.66$$

  The best-fit values are : $|\delta_{32}| = 2.2\times10^{-3}$ eV^2 with $\sin^2\theta_{23} = 0.5$. Whereas δ_{21} is determined to be positive, the sign of δ_{32} is **not** known.

The bound on the mixing angle θ_{13} will require a three generation analysis. The combined analysis of solar, KamLAND, CHOOZ data gives a bound on this parameter. Note however that this bound is sensitive to δ_{32} since the CHOOZ limit on θ_{13} depends sensitively on δ_{32}[23].

- CHOOZ reactor + Atmospheric + Solar + KamLAND experiments[6] : The global data gives the following bound on θ_{13}

$$\sin^2\theta_{13} \le 0.047(3\sigma)$$

  .

- The allowed range of the (small) mass hierarchy parameter, $\alpha = \delta_{\mathrm{sol}}/\delta_{\mathrm{atm}}$

$$0.024 < \alpha < 0.060(3\sigma)$$

  The best-fit value is $\alpha = 0.035$.

Parameter	best-fit	3σ
$\delta_{21}/10^{-5}\text{eV}^2$	8.3	7.2 – 9.1
$\lvert\delta_{32}\rvert/10^{-3}\text{eV}^2$	2.2	1.4 – 3.3
$\sin^2\theta_{12}$	0.30	0.23 – 0.38
$\sin^2\theta_{23}$	0.50	0.34 – 0.68
$\sin^2\theta_{13}$	0.00	≤ 0.047

Table 3.1: Best-fit values and 3σ intervals for three flavour neutrino oscillation parameters from global data including solar, atmospheric, reactor(KamLAND and CHOOZ) and accelerator(K2K) experiments.

The result of the CHOOZ experiment, which requires the U_{e3} element to be small, plays a key role here. It can be shown that this decouples the solar and atmospheric sectors and the three-flavour case almost reduces to separate two-neutrino mixing scenarios at relevant scales to the present day experiments. Due to the small value of θ_{13}, the 2 generation bounds are stable. In table 3.1, we summarise the results of the global three-neutrino analysis.

3.3 Atmospheric Neutrinos

The atmospheric neutrino physics program possible with a magnetised iron tracking calorimeter is substantial. One can observe a clear signal of oscillation by **observing the full oscillation swing**. Also the **precision of the parameters,** δ_{32} **and** θ_{23} can be improved to ≈ 10 %. Broad L/E range (possible with atmospheric neutrinos) offers the opportunity to probe large range of δ_{32}. Among the physics capabilities, are the **sensitivity to matter effects and sign of** δ_{32}. In addition we can use atmospheric neutrinos to **probe CPT invariance** which is a *sacred symmetry* of nature.

The observed zenith angle dependence of muon deficit by SK could be explained well by neutrino oscillations. Nevertheless, various other solutions like neutrino decay and decoherence could also explain the data until very recently. In a recent reanalysis of atmospheric data by SK collaboration, it has recently been reported that the L/E dependence of atmospheric data shows a dip, which strengthens the oscillation argument in order to explain the atmospheric neutrino anomaly and disfavours the other non-oscillation solutions. However we would like to emphasise that **in order to still get a conclusive proof of oscillation with enhanced statistical significance we need a detector which has very good resolution in L/E**. A large magnetised iron calorimeter type detector has very good resolution and will be able to see the L/E dependence of atmospheric neutrino flux much more clearly that other water Cerenkov type detector. We present some calculations to demonstrate these capabilities.

3.3.1 Matter effects in atmospheric μ^-/μ^+ events

The number of muons in an experiment depends on $P_{\mu\mu}$ and $P_{e\mu}$, which are the survival probabilities of ν_μ and conversion of a $\nu_e \rightarrow \nu_\mu$ respectively. We studied the energy and trajectory length ranges where the matter effects are very large. The expected event rates for

μ^- and μ^+ in ICAL were computed using Bartol flux[2] tables[24], a modest muon identification efficiency of 50% and an exposure time of 1000 Kton-Yr. The event rates are calculated for the **E range** $5-10$ **GeV and** L **range** $6000-9700$ **km**. The distribution of the event rates, both in the case of vacuum and matter oscillations are shown in figure 3.1 as function of L/E and L for $\delta_{32} > 0$.

The total number of μ^+ events, in the case of vacuum oscillations is 105 and it changes to 103 on inclusion of matter effects. The total number of μ^- events, in the case of vacuum oscillations is 261 and this reduces to 204 on inclusion of matter effect.

We have a 4σ **signal** for matter effects for neutrino parameters $\delta_{31} = 0.002$ eV^2 and $\sin^2 2\theta_{13} = 0.1$. We estimate that the matter effect will lead to about 2.5σ **signal** for the same δ_{31} and $\sin^2 2\theta_{13} = 0.05$. A systematic study of sensitivity of magnetised iron detectors to matter effects as function of θ_{13} and δ_{31} is underway.

The distribution of the event rates, both in the case of vacuum and matter oscillations are shown in figure 3.2 as function of L/E and L for $\delta_{32} < 0$. A comparison with figure 3.1 immediately shows the impact of hierarchy on the distribution of events when matter effects are included.

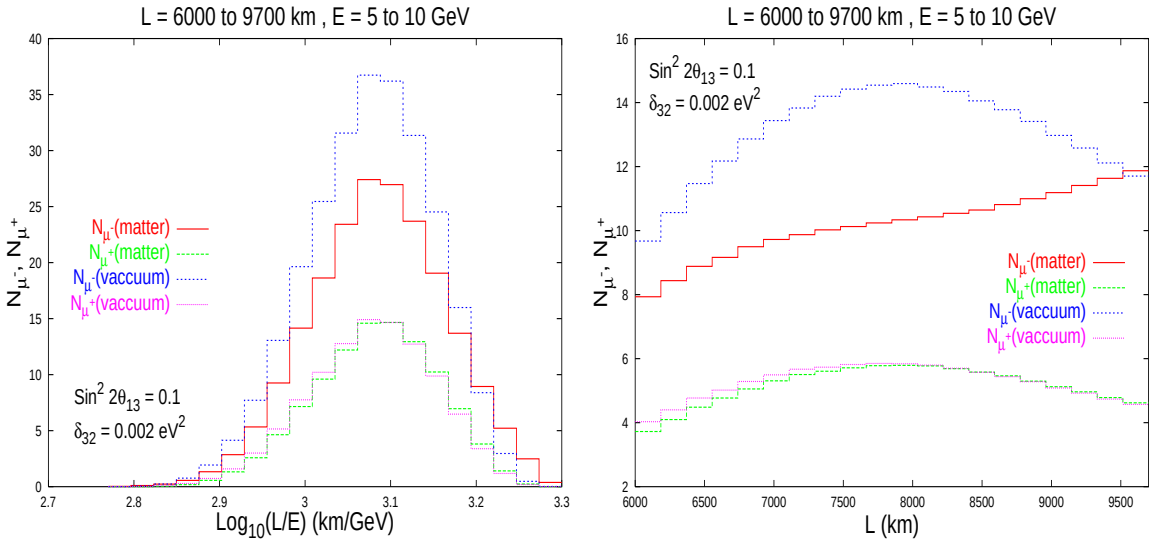

Figure 3.1: Left – The total event rate for muons and anti-muons in matter and in vacuum plotted against $Log_{10}(L/E)$ for the restricted choice of L and E range. Right – The total event rate for muons and anti-muons in matter and in vacuum plotted against L.

Iron Calorimeters with charge discrimination capability have a large range in sensitivity to L/E variations compared to Water Cerenkov detectors and can substantiate the absolute proof of neutrino mass and oscillation already observed by SK, via the observation of dips and peaks in the event-rate vs L/E.

In the following, we have presented the results for L/E sensitivity for such a detector setup. To calculate the event rates in the detector, we have assumed a two neutrino os-

[2]It is expected that the results will not be sensitive to whether Honda[25] or Bartol flux tables are used as long as the ratios of events are involved

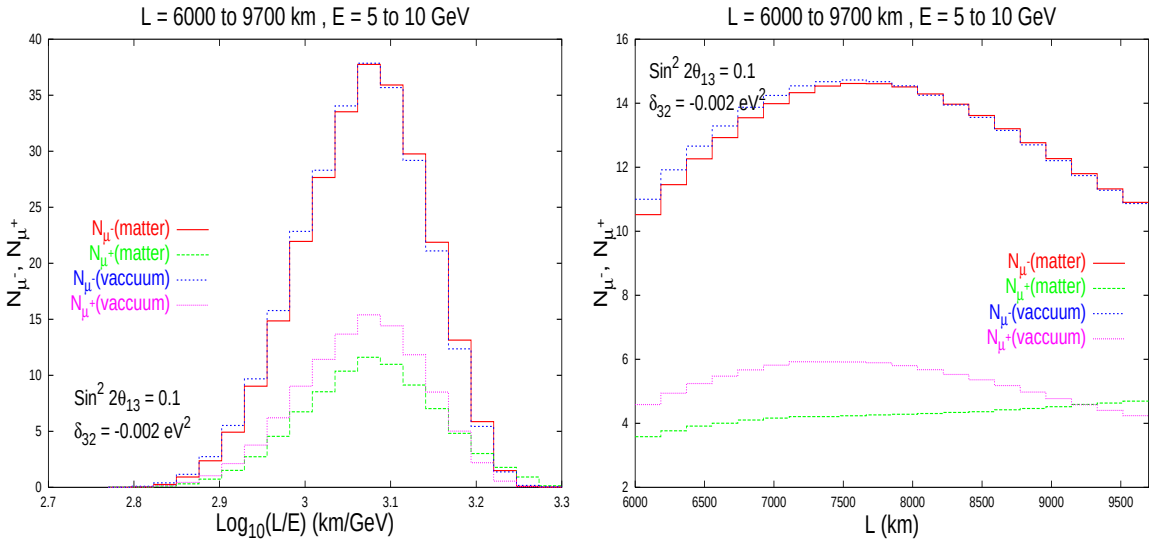

Figure 3.2: Same as figure 3.1, for inverted hierarchy: $\delta_{32} = -0.002\text{ev}^2$.

cillation scenario, instead of full three generation exact formulas for survival probabilities. While this is sufficient to identify clearly the first dip and extract the values of $delta_{32}$ and $\sin(2\theta_{23})$, disentangling matter effects requires the full three generation calculations. This approximation is also quite reasonable in the light of present limits on the mass-square differences from different experiments. To parametrise the effects of smearing due to finite detector resolution we have used the following expression for ν_μ survival probability:

$$P_{\mu\mu} = 1 - \frac{\sin^2(2\theta_{23})}{2}\,[1 - R\,\cos(2.54\,\delta_{32}L/E)] \tag{3.2}$$

where $R \equiv \exp(-0.25\delta_{32}L/E)$.

In Figure 3.3, the number of up- (solid histogram) and down-going (broken histogram) muons (of either sign) in L/E bins are presented for two values of δ_{32}. Positions of dips in L/E bins for up-going case points to the oscillation.

A useful measure of oscillations is the ratio of up-coming to down-going neutrinos with nadir/zenith angles interchanged. The fluxes of atmospheric neutrinos from directions θ and $(\pi - \theta)$ are expected to be similar in the absence of oscillations, especially for larger energies, $E >$ few GeV. Since the path-length traversed, L, is related to θ as

$$L = f(|\cos\theta|) - R\cos\theta\ ,$$

the replacement $\theta \leftrightarrow (\pi - \theta)$ effectively changes the sign of the second term in the equation above. Thus taking, for instance, a down-going neutrino to an up-coming one. The ratio of events in the up-down directions for a given $x = L/E$, therefore, reflects the asymmetry of the up-down fluxes, due to oscillations, and hence is a direct measure of oscillation probability. We define

$$\mathcal{R} = \frac{U}{D}(x) = \frac{\text{No. of events from up-coming muon neutrinos}(x)}{\text{No. of events from down-going muon neutrinos}(\tilde{x})}\ ,$$

Figure 3.4, shows, for same values of δ_{32}, the ratio of up to down going muons in the detector. This ratio, directly connected to the ν_μ survival probability, is thus an important observable. Value of δ_{32} can be determined from the minima and maxima of this ratio. And a good experimental resolution for L/E is extremely important for an accurate determination of δ_{32}.

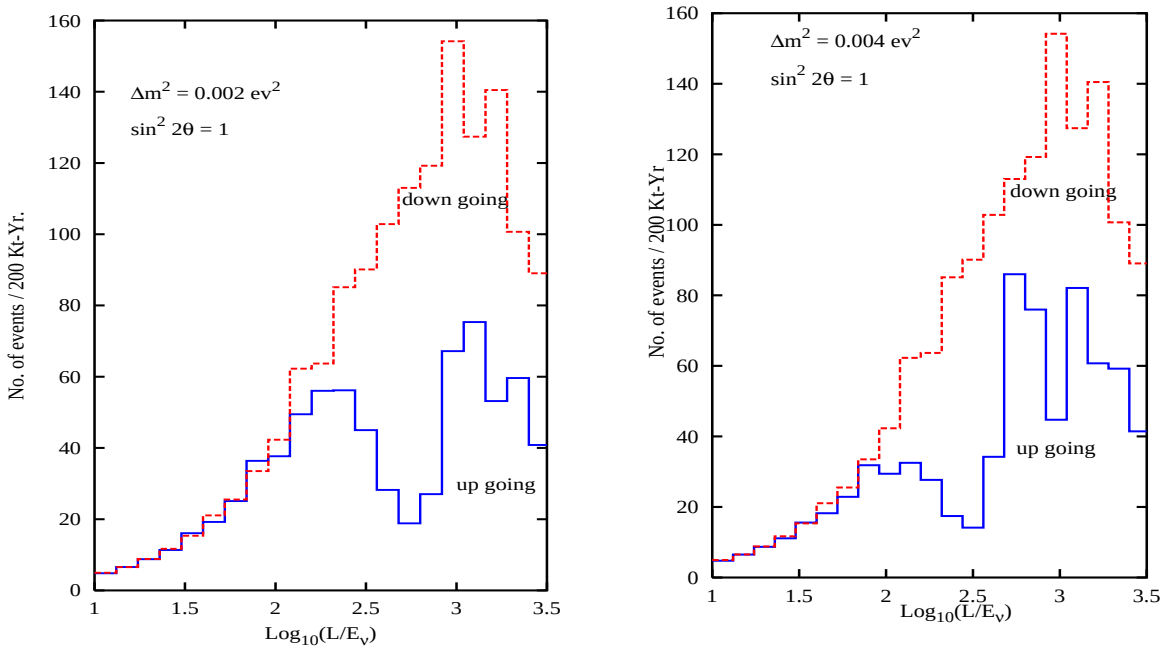

Figure 3.3: The number of up- (solid histogram) and down-going (broken histogram) muons (of either sign) in L/E bins are presented for two values of $\delta_{32} = 0.002, 0.004\text{eV}^2$.

In Figure 3.3, we plot the number of up-going (solid line) and down-going muon plus anti-muon events in each L/E bin, for the δ_{32} and $\sin^2 2\theta_{23}$ values shown, assuming a two generation $\nu_\mu \rightarrow \nu_x$ scenario.

Figure 3.4 shows the ratio of these rates (up going/down going) along with assumed $\sqrt{N}$ errors. The solid line is the best-fit curve. It is clear that the dip and subsequent rise in this quantity should yield firm evidence of oscillations within a few years of data-taking.

The observation of L/E dip can allow us to measure the atmospheric mass-squared difference with a high precision. The spread in δ_{32} is 39% from SK zenith data whereas it is 22% from SK L/E data. Thus with L/E data one gets an improved precision in the measurement of δ_{32}. Range of $\sin^2\theta_{23}$ however is unaffected: $\delta(\sin^2\theta_{23}) \sim 5\%$. However $\delta(\sin^2\theta_{23}) \sim 32\%$ because $\sin^2\theta_{23}$ precision is worse than $\sin^2 2\theta_{23}$ near maximal mixing. Increased statistics in L/E data can improve δ_{32} uncertainty to $\sim 10\%$ at 90% C.L. in 20 years of SK running. This is sensitive to the true value of δ_{32} chosen and the above precision is achieved for $\delta_{32} = 2.5\times10^{-3}$ eV^2. But the precision in $\sin^2\theta_{23}$ doesn't improve with increased statistics. Atmospheric neutrinos and a large magnetised iron calorimeter like MONOLITH, INO[13, 19] can improve the precision of both the atmospheric parameters.

Fig 3.4(right), shown here as a check on the calculations, gives the 68%, 90% and 99% CL contours gleaned from the fits, and shows the best-fit parameter values for δ_{32} and $\sin^2 2\theta_{23}$ returned by MINUIT, which compare very well with our input parameters.

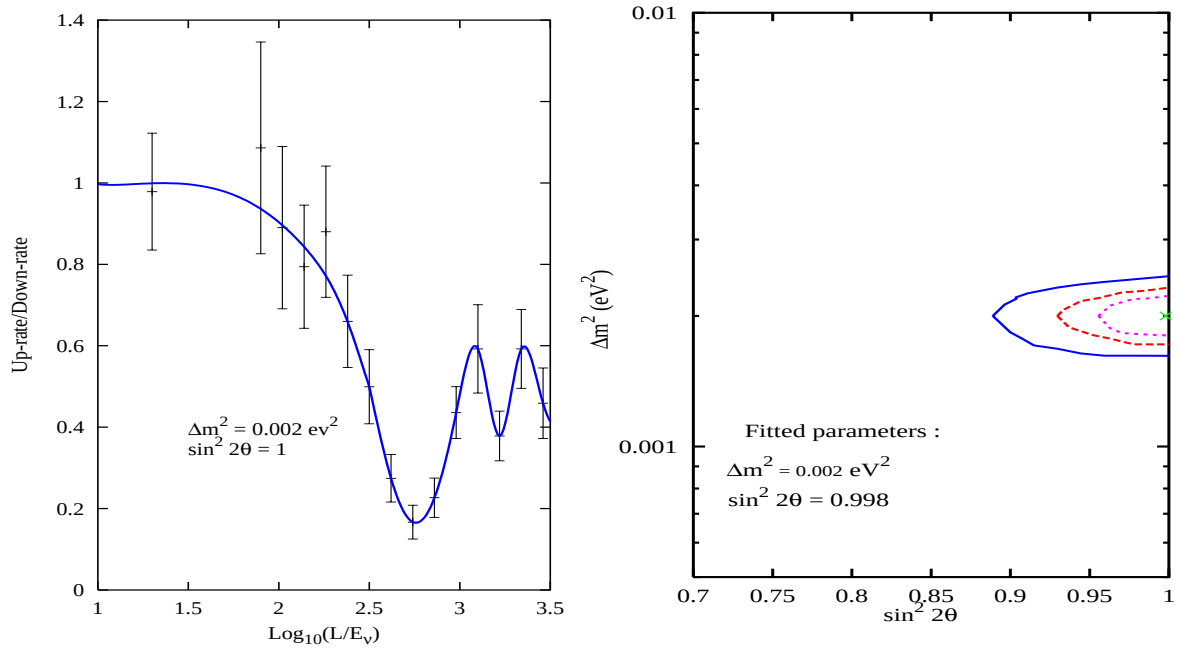

Figure 3.4: Left – The ratio of up to down muon events along with the statistical error bars is plotted against $Log(L/E)$. The solid line is the best-fit curve. Right – The 68%, 90% and 99% CL contours gleaned from the fits. The cross depicts the best-fit parameter values for δ_{32} and $\sin^2 2\theta_{23}$.

3.3.2 The question of hierarchy– Sign of δ_{32}

Apart from the observation of the actual oscillation pattern to a better precision as shown above, it has been recently realised that the magnetised iron calorimetric detector (ICAL), with its ability to detect the charge, may be in position to resolve an outstanding problem, namely, **sign of** δ_{32} often referred to as the **Hierarchy Problem** using atmospheric neutrinos instead of waiting for the long-baseline neutrino beams to materialise[26].

As is clear from figures 3.1 and 3.2 the earth matter effects are not the same for neutrinos and antineutrinos. The neutrino and anti-neutrino up/down event ratios are different from each other as well as different with direct($\delta_{32} > 0$) and inverted ($\delta_{32} < 0$) mass hierarchies (due to matter effects); the distinction (and hence measurement possibilities) between the two hierarchies can be amplified by defining the asymmetry,

$$\mathcal{A}_N(x) = \frac{U}{D}(x) - \frac{\overline{U}}{\overline{D}}(x) \ , \tag{3.3}$$

where x denotes the appropriate choice of variable to study the asymmetry (we choose this to be L/E) and $U(\overline{U})$ denotes the up-going events for neutrinos (antineutrinos) and $D(\overline{D})$ denotes the down-going events for neutrinos(antineutrinos) respectively.

The asymmetry, calculated numerically, and integrated over $E_{\rm min} > 4$ GeV is plotted as a function of L/E in Fig. 3.5 for $|\delta_{32}| = 1, 2, 3 \times 10^{-3}$ eV^2. The thick (blue) curves in the figure correspond to the direct mass hierarchy (labelled D) and the thin (red) curves to the inverted mass hierarchy (labelled I). The curves in each envelope correspond to $\theta_{13} = 5, 7, 9, 11$ degrees

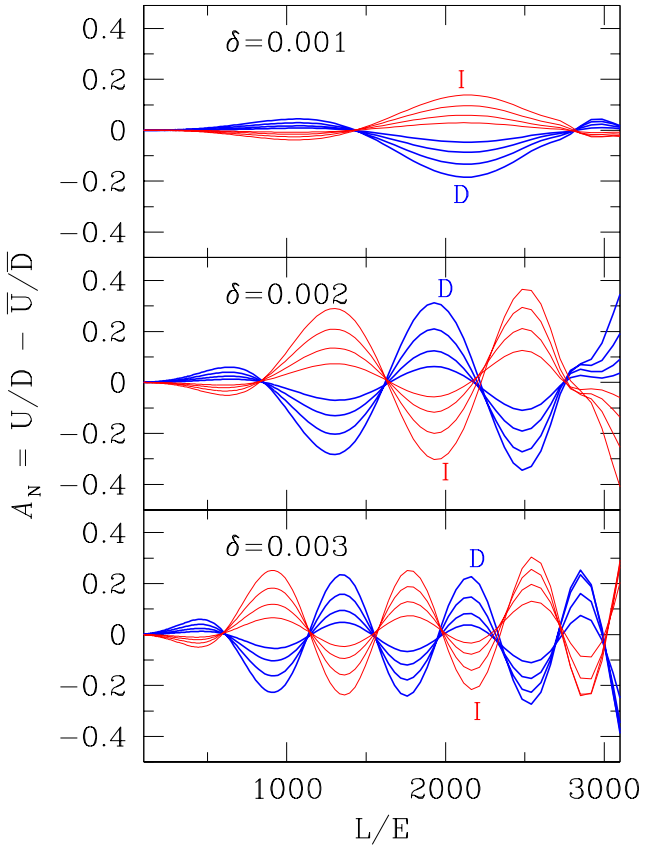

Figure 3.5: The difference asymmetry (difference of up/down ratios of muon neutrinos and antineutrinos) as a function of L/E for $E > 4$ GeV. The three panels correspond to $\delta \equiv |\delta_{32}| = 1, 2, 3 \times 10^{-3}$ eV^2. The thick (blue) curves correspond to the direct $\delta_{32} > 0$ and the thin (red) curves correspond to the inverse $\delta_{32} < 0$ hierarchy. The innermost curve in each envelope corresponds to $\theta_{13} = 5°$ and the outermost corresponds to $\theta_{13} = 11°$ with 7° and 9° in between. For other parameters the best fit values given in the text are chosen.

($\sin^2 2\theta_{13}$ from 0.03–0.14) with the asymmetry increasing symmetrically with θ_{13} about the $\mathcal{A}_N = 0$ line for direct and inverse hierarchies. It is seen that the direct and inverted asymmetries are exactly out of phase. The maximum divergence between the direct and inverted hierarchies is smaller in the first envelope than in the second; these correspond to the first dip and rise in the up/down events ratio.

Detailed analysis shows that the set of measurements required for resolving the hierarchy problem may need about **1000 kton-Years** of exposure given the resolution in energy and zenith angle at present provided $\theta_{13} > 6$ degrees. With better resolution for both energy and direction (than has been achieved at present) of the atmospheric neutrinos and antineutrinos it may be possible to bring the exposure down to about 500 kton-years. Detailed calculations are in progress.

3.3.3 Discrimination between the $\nu_\mu \to \nu_\tau$ and the $\nu_\mu \to \nu_s$

The ICAL detector also provides a new way of distinguishing whether the muon neutrino deficit observed by previous experiments is due to oscillations of muon neutrinos to tau

neutrinos or to sterile ones. If the dominant oscillation is $\nu_\mu \rightarrow \nu_\tau$, as appears probable from SK data, then there will be charged current (CC) production of τ leptons in the detector, originating from the ν_τ produced due to these oscillations. At these energies, the τ lepton decays very rapidly, and roughly 80% of the time this decay does *not* produce a muon.

The visible hadronic activity generated in these events has the appearance (if specific cuts for τ detection are not designed) of a neutral-current (NC) event due to the lack of a visible lepton charged track. Thus this oscillation scenario significantly alters the up/down ratio of the "muon-less" events when compared to the $\nu_\mu \rightarrow \nu_s$ possibility. In fact, the asymmetry in the ratio assumes positive values in one case ($\nu_\mu \rightarrow \nu_\tau$) and negative values in the other ($\nu_\mu \rightarrow \nu_s$), since the upward rate is enhanced significantly by CC τ events (which appear as "fake" NC events) in the former case, but depleted if the oscillation is to sterile neutrinos since they will have neither CC nor NC interactions.

Figure 3.6 quantifies this, where we show the ratio of the asymmetry in the rates for two different values of δ_{32}, for both possible modes of oscillation. Note also the relative difference visible for both these values, showing that this provides an independent handle on the value of this parameter, in addition to the sensitivity discussed in the CC mode above.

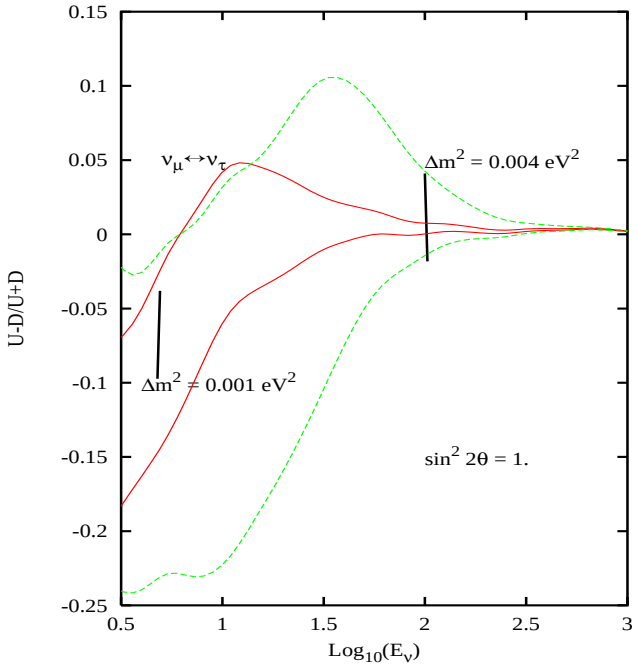

Figure 3.6: Ratio of asymmetry plotted against E (GeV) for different values of δ_{32}, for both possible modes of oscillation, $\nu_\mu \rightarrow \nu_\tau$ and $\nu_\mu \rightarrow \nu_s$.

3.3.4 Probing CPT Violation

It has been proposed that the atmospheric neutrinos in conjunction with ICAL may also be used as a probe of the level of Lorentz and CPT violation[27]. The survival probabilities for neutrinos and antineutrinos, in a two flavour scenario, are identical. However in presence of the effective **C- and CPT-odd interaction** terms $\bar{\nu}_L^\alpha b_{\alpha\beta}^\mu \gamma_\mu \nu_L^\beta$, where α and β are flavour

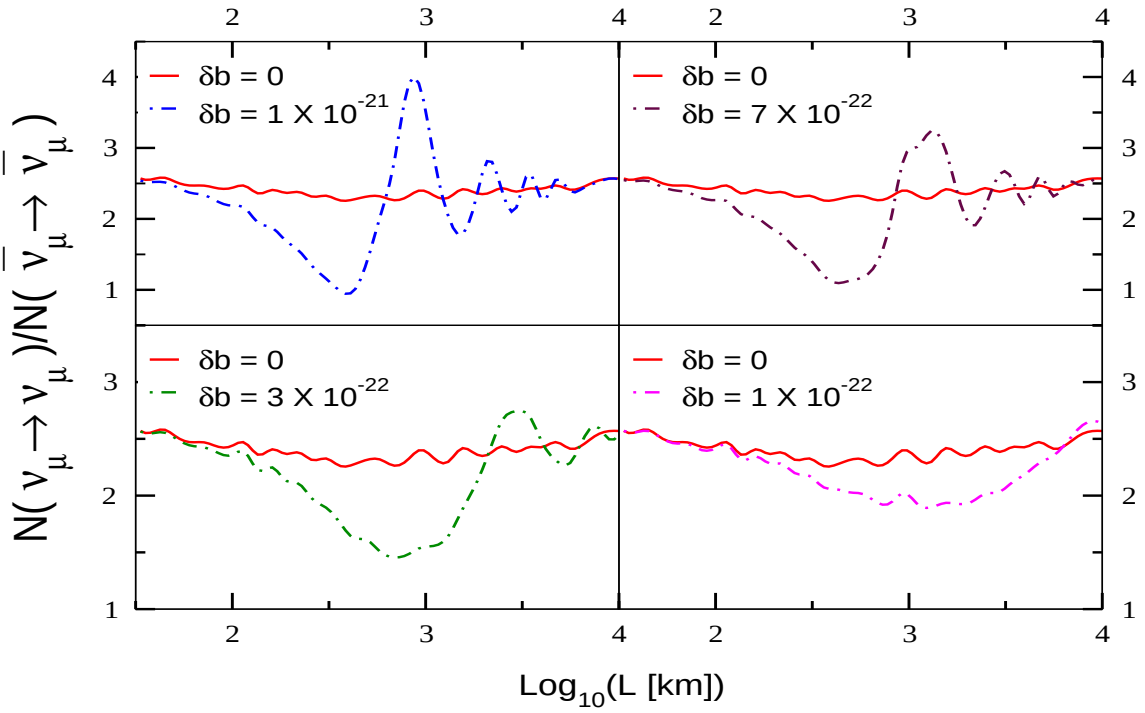

Figure 3.7: The ratio of total (up+down) muon to anti-muon events plotted against $Log_{10}(L)$ for different values of δb (in GeV). The oscillation parameters used in all the plots $\delta_{32} = 2 \times 10^{-3}$ eV^2 and $\sin^2 2\theta_{23} = 1$.

indices, the expression for survival probability is

$$\mathrm{P}_{\mu\mu}(\mathrm{L}) = 1 - \sin^2 2\theta \, \sin^2 \left[\left(\frac{\delta_{32}}{4\mathrm{E}} + \frac{\delta \mathrm{b}}{2} \right) \mathrm{L} \right] \tag{3.4}$$

where δ_{32} and δb are the differences between the eigenvalues of the matrices m^2 and b, respectively. Note that δb has units of energy (GeV). Thus one could define an asymmetry

$$\Delta \mathrm{P}^{\mathrm{CPT}}_{\mu\mu} = P_{\mu\mu} - P_{\bar{\mu}\bar{\mu}} = -\sin^2 2\theta \, \sin \left(\frac{\delta_{32} \mathrm{L}}{2\mathrm{E}} \right) \sin(\delta \mathrm{bL}) \tag{3.5}$$

Observable CPTV in 2 flavour case is a consequence of interference of the CPT-even and CPT-odd terms. We focus on the survival probabilities for ν_μ and $\bar{\nu}_\mu$ which are a measure of these violations.

In Figure 3.7, we plot the ratio of muon to anti-muon events vs L using Bartol atmospheric neutrino flux. We show that (by studying the variation with L), it is possible to detect the *presence* and also obtain a *measure of the magnitude* of δb by studying their minima and zeros for $\delta \mathrm{b} \geq 3 \times 10^{-22}$ GeV. For some what lower values of δb (but $\geq 3 \times 10^{-23}$ GeV), the plots vs L/E indicate only the *presence* of CPTV without the same discriminating capability. The bounds that we have obtained compare very favourably with those obtained from neutrino factory[28]. We note that the value of δb compares with $\delta_{32}/2\mathrm{E} \approx 10^{-21}$ GeV. Our calculations indicate that an exposure of **400 kT-yr** would be sufficient for statistically significant signals to emerge.

3.3.5 Constraining long-range leptonic forces

Long range forces in the context of particle physics originated with the ideas of Yang and Lee and Okun[29] who proposed that gauging the baryon number or lepton number would give rise to a composition dependent long range force which could be tested in the classic Eotovos type experiments. A special class of long range forces which distinguish between leptonic flavours have far reaching implications for the neutrino oscillations which may be used as a probe of such forces.

The leptonic long range forces which distinguish between their flavours have been shown to significantly influence the oscillations of the atmospheric, solar as well as terrestrial neutrinos. The potential generated by these forces distinguishes between neutrino and anti neutrino. Thus the magnetised iron calorimeter, ICAL, which can distinguish the muon charges could provide more sensitive test of these forces. Detailed analysis in case of the atmospheric neutrinos shows that such detectors have the potential to further improve bounds on the long range couplings by an order of magnitude[30].

3.4 Neutrino Factories

The possibility of neutrino beams from muon storage rings has received a lot of attention in the recent literature[31]. Such facilities provide intense, controlled high luminosity neutrino beams that are almost pure $\nu_\mu + \bar{\nu_e}$ or $\nu_e + \bar{\nu_\mu}$ depending on the sign of the stored muon. With its charge discrimination capability, a magnetised iron calorimeter offers unique capabilities to exploit the physics potential of such sources.

As is well understood by now, these kind of high purity high intensity neutrino beams may provide the best and cleanest, if not the only way to achieve at least three goals mentioned above. While the determination of mass hierarchy seems to be rather straight forward, determination of θ_{13} and δ are sensitive to the baseline chosen. Many neutrino factory locations and corresponding end-detector sites are under consideration and active discussion all around the world. In what follows, we explore the physics discovery potential of a ICAL at INO, when used as an end detector for a neutrino factory beam originating from the Japan Hadron Facility at Jaeri (JHF) and another from Fermilab, USA. There are two possible locations in India. One is at *PUSHEP* in southern part of India. The other one is at *Rammam* in north-eastern part. We will consider in the following, the four possible baseline lengths. The baseline lengths corresponding to these sites are as follows: *JHF–Rammam*: 4865 km; *JHF–PUSHEP*: 6591 km; *Fermilab–Rammam*: 10489 km and *Fermilab–PUSHEP*: 11296 km.

3.4.1 Determination of θ_{13}

The first set of calculations we have performed explore the reach for θ_{13}. We recall that the CHOOZ bound on this parameter is $sin^2 2\theta_{13} < 0.1$. Its importance lies in it being the driving parameter for $\nu_e \rightarrow \nu_\mu$ oscillations, and for CP violation searches. We stress that this is true with or without matter effects. The next generation of experiments will thus have its determination as one of the primary goals.

Figure 3.9 demonstrates the achievable values of $\sin\theta_{13}$ versus the muon detection threshold energy of the detector. The reach is determined as the value which is necessary to collect 10 signal events (that is events that involve wrong sign muons) for a given kT-yr exposure.

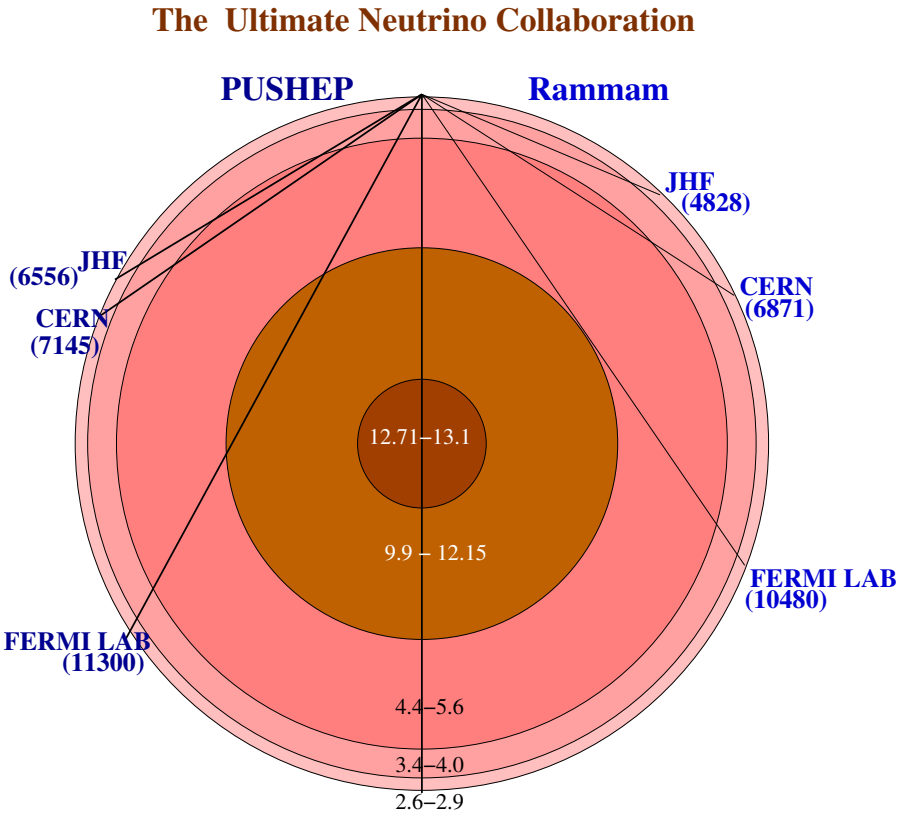

Figure 3.8: Baselengths (kms) from the proposed neutrino factories to the two proposed INO sites in India: Left half shows the baselengths to the site at PUSHEP whereas the right-half shows the baselengths to the site at Rammam. The densities of the layers that the neutrinos pass through are also indicated.

We show the reach capabilities for an entry-level configuration ($E_\mu^{th} = 20$ GeV, 10^{19} decays per year). For the median detector size of 50 kT running for 1 year, at a muon detection threshold of 2 GeV, the reach corresponds to $\sin\theta_{13} = 0.038$ or $\sin^2 2\theta_{13} = 0.0057$ for *Rammam* and a slightly higher value for *PUSHEP*, as shown. The *reach* values improve to $\sin\theta_{13} = 0.026$ or $\sin^2 2\theta_{13} = 0.0027$ for *Rammam* if the energy of the beam is increased to 50 GeV, keeping other variables the same as before. In all of the above, the "passive" parameters $\delta_{32}, \delta_{21}, \sin^2 2\theta_{23}$ and $\sin^2 2\theta_{12}$ are held to their (best-fit) values specified above.

A second method of obtaining a *measure* of θ_{13} is via matter effects which show up once the baselines are long. In particular, the total right-sign muon rate varies measurably with θ_{13}, as demonstrated in Figure 3.10 for the *JHF-PUSHEP* baseline. Here the number of such events are shown as a function of E_ν/δ_{32} for a neutrino factory with 10^{21} muon decays/yr. Clearly, a measure of this important parameter, even if it is small, is possible via this method. Note that the event-rate peaks nicely for neutrinos in the 10-20 GeV range for the currently allowed and favoured range of values of δ_{32} from atmospheric neutrino data.

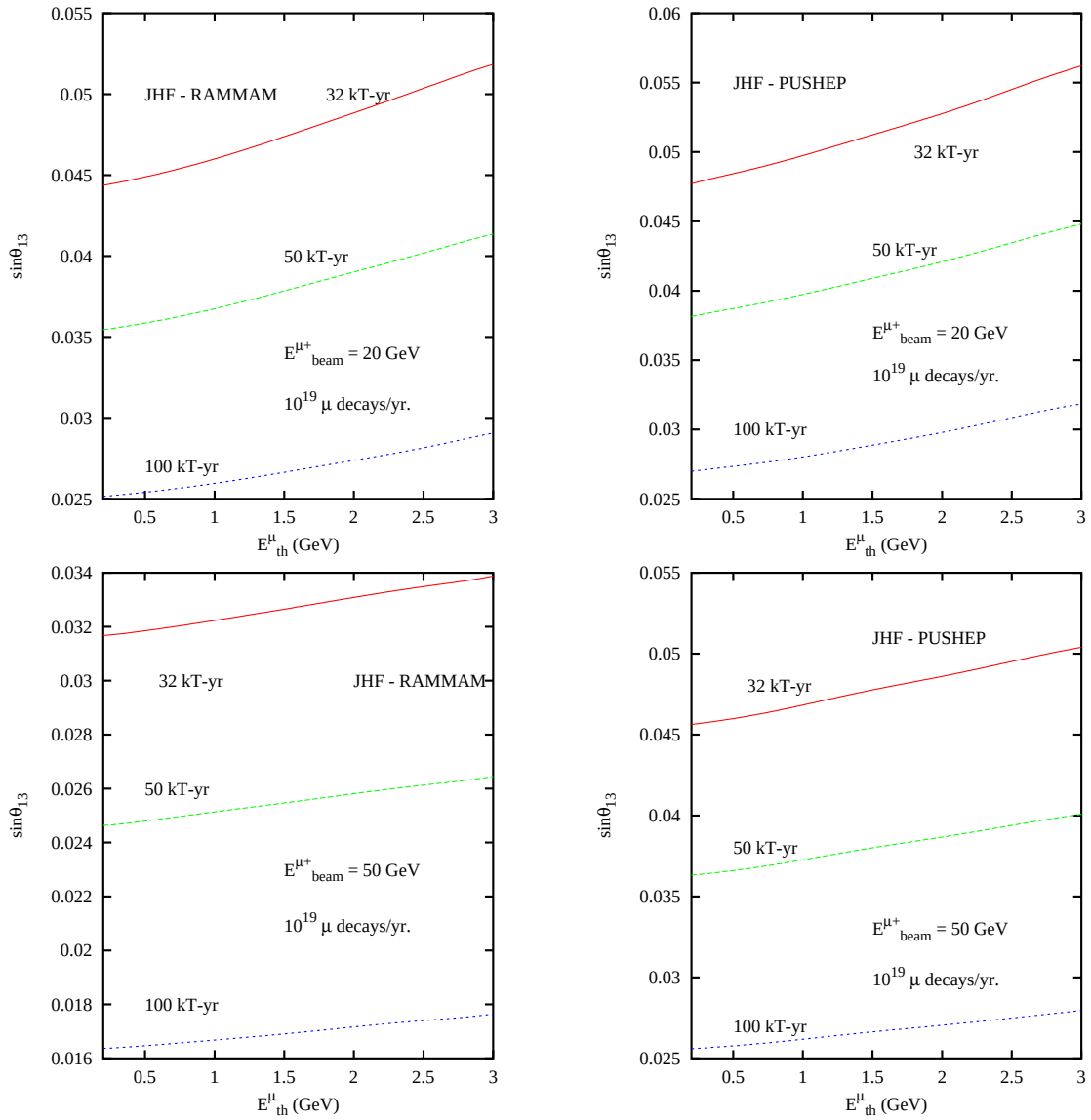

Figure 3.9: The $\sin\theta_{13}$ reach for detector exposures of 32 kT-yr, 50 kT-yr and 100 kT-yr for an entry-level neutrino factory configuration with $E_\mu = 20$ GeV for the (a) JHF-RAMMAM baseline, the JHF-PUSHEP baseline (b). In (c) and (d) we show the improvement in reach if the storage muon energy is increased to 50 GeV, keeping the number of decays per year the same, i.e, 10^{19}/yr.

3.4.2 Sign of δ_{32}

We next examine the capability to determine the sign of E_ν/δ_{32} that these baselines offer. This is sensitive once again to the wrong-sign muon rate generated by $\nu_e \to \nu_\mu$ oscillations. For small θ_{13}, and if the matter potential $A \sim E_\nu/\delta_{32} > 0$, then matter effects lead to an enhancement of $\nu_e \to \nu_\mu$ and a suppression of $\bar{\nu_e} \to \bar{\nu_\mu}$. The converse is true if the sign of $A \sim E_\nu/\delta_{32}$ is reversed.

Figure 3.11 shows the sign discrimination capability for an entry-level neutrino factory configuration with a 32 kT detector running for a year. For both the *Rammam* and *PUSHEP* baselines, the sign dependent difference in event rates is easily measurable in terms of wrong sign muon events. For comparison, we also show the difference in event-rates for a JHF-

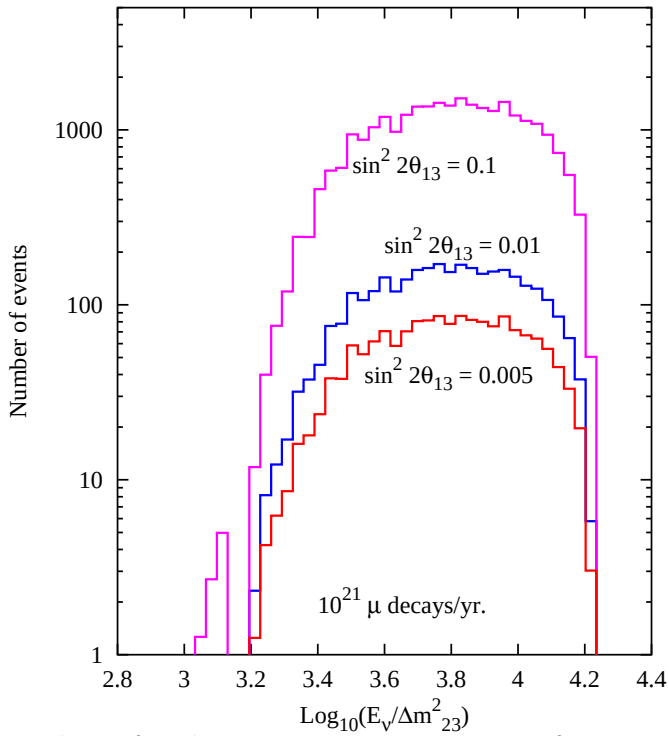

Figure 3.10: The number of right-sign muon events as a function of E_ν/δ_{32} for the JHF-PUSHEP baseline. The dip to the left of the distribution is due to a minimum of the oscillation probability.

China baseline (1952 km) were a similar detector to be set up there. Figure 3.12 shows the improvement (or rather, the overkill) possible with a upgraded factory yielding 10^{21} decays per year with a beam energy of 50 GeV running for one year, with the detector mass increased to 50 kT.

3.4.3 Probing CP violation in leptonic sector

We next examine the discovery potential for what many consider as the holy grail of physics in the lepton sector, i.e. the presence or absence of CP violation. In the standard three generation scenario, this is parametrised by a single phase δ in the lepton mixing matrix. In principle, rates for particles and their CP conjugates will exhibit a difference stemming from terms proportional to $\sin\delta$ in the oscillation probability. Generally, these differences are small and difficult to dis-entangle from matter oscillation effects, which in long baseline situations dominate differences due to CP. The detectability depends sensitively on $\sin^2 2\theta_{13}, \delta_{21}$, the energy and baseline, among other parameters, besides of course on the magnitude of $\sin\delta$.

One possible clean signature is the ratio of wrong sign muon events for equal exposures when the neutrino factory runs with muons and anti-muons stored in the ring in turn. Thus for negatively charged stored muons, one expects $\bar{\nu_e} \to \bar{\nu_\mu}$ oscillations to produce CC induced positively charged muons, and vice-versa for a run with stored μ^+ in the ring.

In Figure 3.13(a), we show (as a function of baseline length)the ratio of wrong-sign muon events for a run with negatively charged muons in the storage ring (and, hence, the resultant μ^+ events due to oscillations, denoted by $N(\mu^+)$) to that for a run with positively charged muons (yielding μ^- events via oscillations, denoted by $N(\mu^-)$). The calculations are performed for a factory with a beam energy of 20 GeV and a muon decay yield of 10^{21} decays per year. For this plot a value of $\sin\theta_{13} = 0.1$ ($\sin^2 2\theta_{13} = 0.04$) has been assumed,

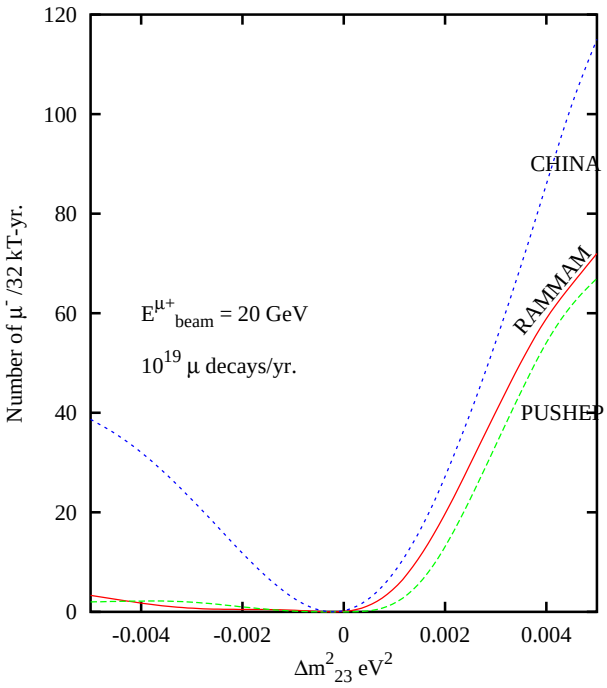

Figure 3.11: The number of wrong-sign muon events as a function of δ_{32} for the three baselines from JHF, demonstrating the sign discriminating capability which arises as a result of matter effects. Event rates are computed for an entry-level configuration with a 32 kT-yr exposure, beam energy of 20 GeV and 10^{19} decays per yr.

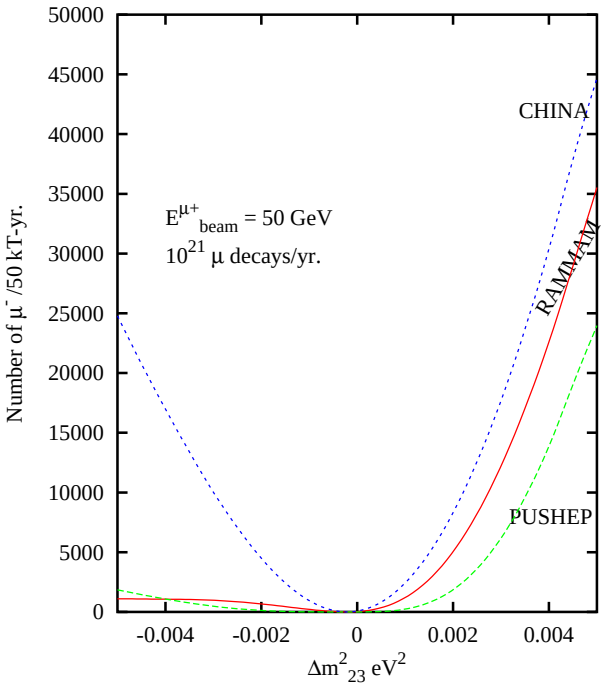

Figure 3.12: The same as Figure 3.11, but for a upgraded neutrino factory configuration with a 50 kT-yr exposure, 10^{21} decays per yr and a beam energy of 50 GeV.

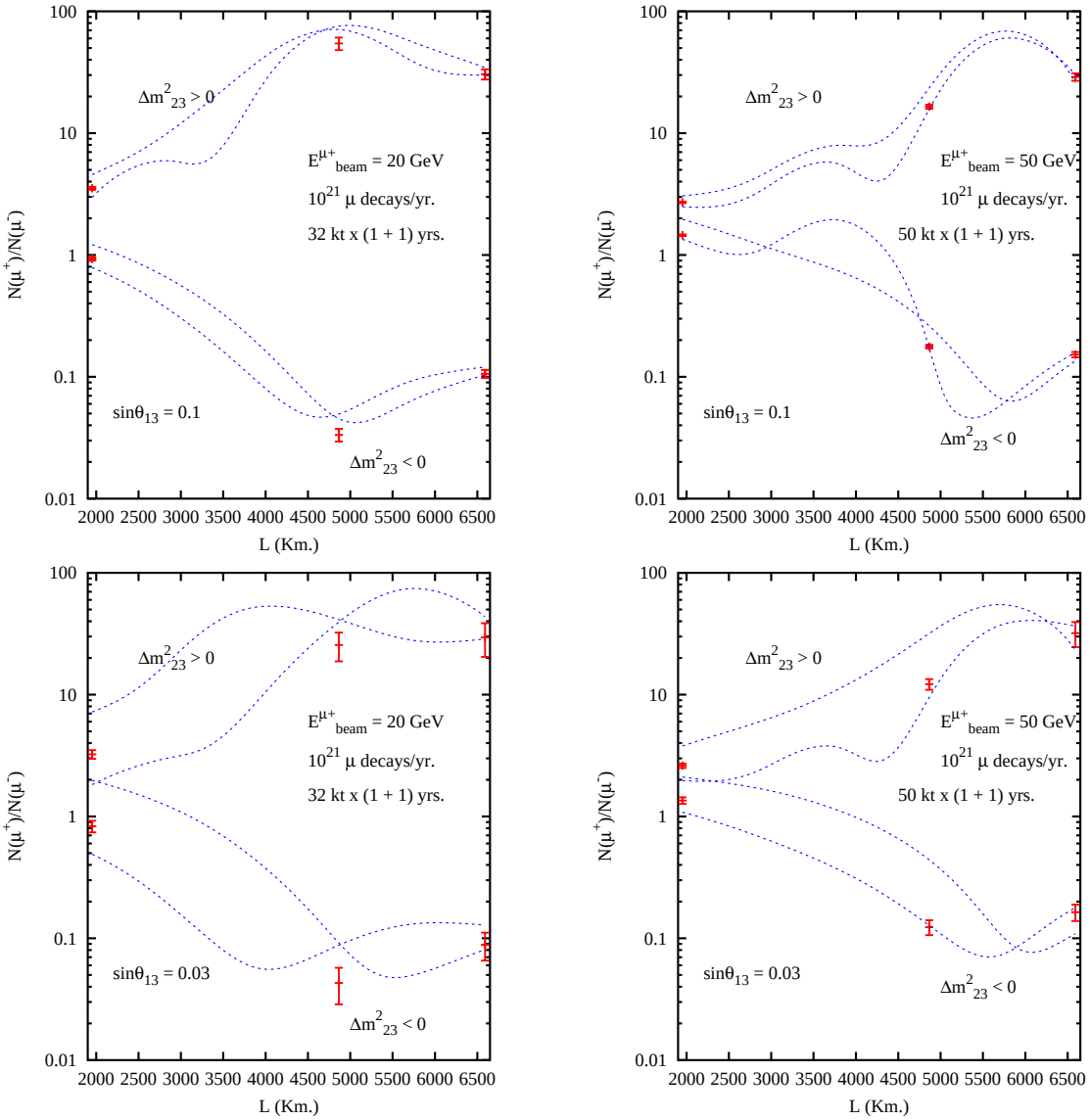

Figure 3.13: The ratio of wrong-sign muon events for equal-time runs of opposite sign muons and $\delta = \pm\pi/2$ (dashed curves) and $\delta = 0$ (data points) in the storage ring, versus baseline length. The top row shows the results for $sin\theta_{13} = 0.1$ ($sin^2 2\theta_{13} = 0.04$) and 10^{21} decays per year, with beam energies of 20 GeV in one case and 50 GeV in the other. The bottom row shows the results when $sin\theta_{13} = 0.03$ ($sin^2 2\theta_{13} = 0.0036$). The positions of the data points reflect the baseline lengths for detector locations at Beijing, Rammam and PUSHEP in order of increasing length.

along with a run of 1 year each of either sign of stored muon, and a detector mass of 32 kT has been used. The dashed curves are for $\delta = \pm\pi/2$ and the data points show the values (along with statistical errors) for $\delta = 0$ at the Beijing , *Rammam* and *PUSHEP* respectively. The two sets of curves (upper and lower) correspond to opposite signs of δ_{32}, which reflect the effects of matter. We note that CP effects tend to cancel (i.e are small) for this configuration at *PUSHEP*, hence the measurements there afford an opportunity to effectively isolate and measure the matter effects. Such measurements can be used in conjunction with measurements at a baseline where CP effects are relatively large and afford a cleaner discrimination between $\delta = 0$ and a non-zero value of this parameter. This is

exemplified in Figure 3.13(b) which uses the same parameters as 3.13(a) but assumes a beam energy of 50 GeV and a slightly more massive detector of 50 kT. One notes here (as in Fig 3.13(a)) that the Rammam baseline offers an opportunity to detect the presence of a δ which is different from zero, especially as exposure (in kT-yr) and statistics improve.

Figures 3.13(c) and 3.13(d) show the CP capabilities for the same two configurations as the ones in Fig 3.13(a) and Fig 3.13(b) respectively, but for a lower value of $\sin\theta_{13}$, namely 0.03. Note that both our chosen values of this parameter are well below the current CHOOZ bound. The conclusions for both Rammam and sl PUSHEP are similar to the ones above. The former provides us with an opportunity to measure the presence of a non-zero CP violation, while the latter provides us an opportunity to separate matter effects from the CP violation contributions in conjunction with another long-baseline experiment.

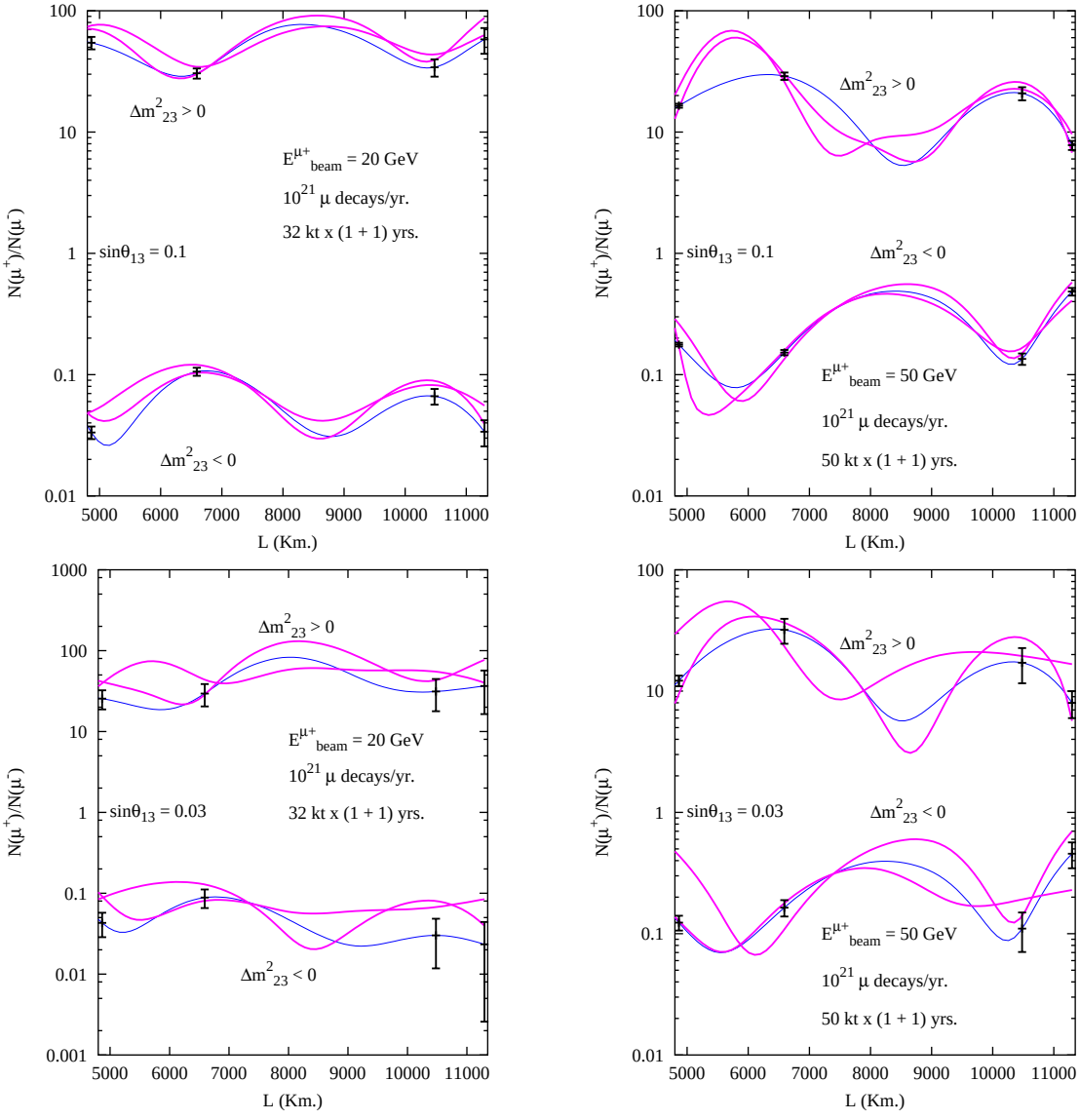

Figure 3.14: Same as Fig.3.13, but for baselines corresponding to Fermilab-PUSHEP, Fermilab-RAMMAM along with same ratios for JHF to two proposed Indian sites. All other parameters are indicated in the plots. The purple lines are for $\delta = \pm\pi/2$. The data points are for $\delta = 0$

Finally in fig.3.14, we have presented the CP capabilities, for baseline lengths correspond-

ing to Fermilab to *PUSHEP* and Fermilab to *Rammam*. The input parameters remain the same as the other set of plots. For comparison we have presented the same numbers for the baselines corresponding to JHF-*Rammam* and JHF-*PUSHEP* again.

3.4.4 Detecting Large Matter Effects in $\nu_\mu \to \nu_\tau$ Oscillations

The $\nu_\mu \to \nu_\tau$ oscillation probability $P_{\mu\tau}$ can also undergo significant change (a reduction as high as $\sim 70\%$ or an increase of $\sim 15\%$) compared to its vacuum values over an observably broad band in energies and baselines due to matter effects. Maximal effect in $\nu_\mu \to \nu_\tau$ oscillations occurs at **L $\sim$ 9700 km, 9300 km, 9900 km for** $\sin^2 2\theta_{13} = 0.05, 0.1$ **and** 0.2 **respectively.** This can also induce appreciable changes in the the muon neutrino survival probability $P_{\mu\mu}$ in matter[32]. For $\nu_\mu \to \nu_\mu$, the effect is maximal at **7000 km for** $\sin^2 2\theta_{13} =$ 0.1. The τ appearance rate as a signal for matter effects can also be searched for in special τ detectors being thought of for neutrino factories. Similarly, detectors capable of measuring muon survival rates[33], e.g. ICAL can detect the effects visible in the bottom panels of Fig. 3.15(a) and (b) at neutrino factories. Typical baselines from existing and proposed neutrino factories to two possible sites in India for INO include $L \sim 7000$ km (*CERN-PUSHEP* and *CERN-Rammam*). Also baselines $L \sim 10500$ km are possible for (*Fermilab-PUSHEP* and *Fermilab-Rammam*) and these are well within the range of baselines where these effects are large and observable. Detailed calculations are in progress.

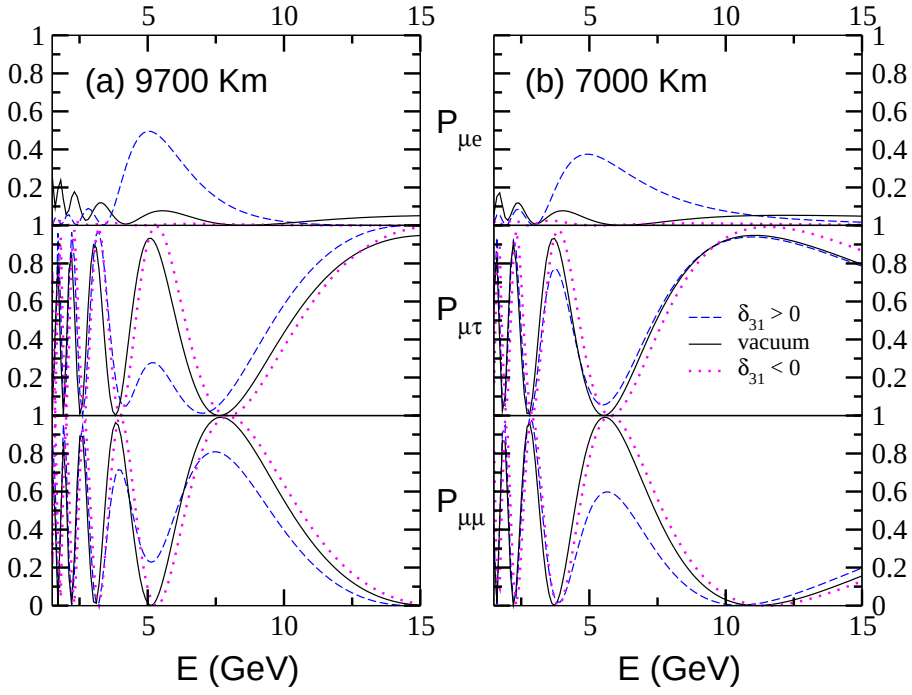

Figure 3.15: $P_{\mu e}$,$P_{\mu\tau}$ and $P_{\mu\mu}$ plotted versus neutrino energy,E (in GeV) in matter and in vacuum for both signs of δm^2_{31} for two different baseline lengths, (a) for L = 9700 km and (b) for L = 7000 km. These plots use $\delta_{31} = 0.002$ eV^2 and $\sin^2 2\theta_{13} = 0.1$.

3.5 Other Physics Possibilities

Kolar events : Earlier experiments at KGF had recorded unusual events[17] indicating the possibility of a long-lived particle with a large production rate. This phenomenon is as yet not well understood. The proposed detector ICAL at INO will be capable of observing many more such events leading to a better understanding and possibly clarifying the origin of these unusual events. We discuss these events briefly below:

In the neutrino experiments at 7000 mwe, as well as those conducted later at 3375 mwe and the proton decay experiments in KGF mines, it was noticed (Krishanamurthy et. al.) that some multi-track events (6 in total) had unusual features which could not be explained away by any known processes of muons or neutrinos. They are characterised by the following features :

- The event consisted of two or more tracks, with at least one of them a muon or a pion as seen from their penetrating power without showering.
- All the tracks of the event seemed to originate from a vertex located either in air or thin detector materials - based on an extrapolation of projected angles of tracks.
- The tracks had a large opening angle ($\sim 45^\circ$) between them, and
- Their rate was depth-independent and was a good fraction of neutrino events.

A number of theoretical attempts were made to understand the production processes[35] and see if they could fit into the prevailing schemes of particles and their interactions. The Kolar events have so far remained an enigmatic puzzle and they need to be studied with specially designed detectors that can address their special characteristics.

Ultra high energy neutrinos and muons : The solar neutrinos have confirmed the basic hypothesis of stellar energy generation, while handful of neutrinos from supernova SN1987A have shed insight into the mechanism responsible for supernova explosions. In a similar manner it may be possible to study of the interiors of other astronomical objects like the Active Galactic Nuclei (AGN) through a study of (high energy) neutrinos from these objects. The phenomenon of Gamma Ray Bursts (GRB) suggests the possibility of the existences of such sources. Thus Neutrino Astronomy opens up of a new window to the Universe and is likely to throw up new, unexpected phenomena. This has happened many times throughout history. Neutrino astronomy is an exciting new field with plenty of scope for surprises.

Detectors like ICAL can also be utilised to study multi-TeV cosmic ray muons through the so called pair meter technique. Such studies in the TeV–PeV regions can throw light on possible extensions of the standard model in the high energy region.

Calculations are in progress to determine the number events at ICAL due to these UHE neutrinos and their signatures. The motivation here is to study the knee in the cosmic ray primary spectrum. Cosmic rays are observed in a wide range of energies. The differential cosmic ray (CR) spectrum is a function of energy with a power law with index -2.7 up to an energy of $\simeq 4 - 7 \times 10^{15}$ eV. This point is called the *knee* in the energy spectrum of CR. Beyond the knee it exhibits a different power law with index -3.1 up to an energy of $\simeq 5 \times 10^{18}$ eV. This change in the behaviour of CR spectrum at the knee poses a puzzle

which can be resolved in two ways. One way is to consider a different composition in the CR spectrum at the knee energy or above.

A second way is to look for the missing energy taken by the undetected particles produced at the knee. The known particles responsible for carrying the missing energy are neutrinos and muons. Existing detectors do not measure the energy of these particles and only count their numbers in CR showers. However with detectors like ICAL one would be able to measure the energies of these muons using pair meter technique. Using this technique one can estimate the event rate of muons for a few years running time, number of interactions, energy of these high energy muons, etc. Calculations of this are underway.

Nucleon decay : One of the most important quests in all of physics remains the search for nucleon decay. Its observation (or lack thereof) provides signatures of physics at the unification scale, not accessible to accelerator experiments. The present best limits on the mode $p \rightarrow e^{+}\pi^{0}$ are a lifetime of 3×10^{34} years (from SK). Many SUSY GUT models favour nucleon decay modes with K mesons, which have atmospheric neutrino background, for which the limit from SK will be roughly the same. Current expectations from theory range over several orders of magnitude above this limit, but nucleon decay could well be found at a life time longer than 10^{35} years. Such a limit may be tested with a megaton detector. This can not be done by the present ICAL detector but remains a distinct possibility as a future experiment at INO.

Chapter 4

Tale of two (three) sites

An important component of the INO feasibility study would be to find an appropriate location with sufficient rock overburden to satisfy the physics objectives. This section outlines the results of the various surveys undertaken in many places all over the country. This has been necessitated by the fact that one of the best sites available in the world, namely KGF, is not accessible for experiments any more. We first outline the set of criteria which were used to determine the suitability of the sites surveyed for the location of INO.

The site survey group studied the topographic material, discussed with the scientists of the Geological Survey of India and the engineers involved in many underground projects, regarding many possible sites in the Western Ghats of South India, the lower Himalayan region in West Bengal. Based on a set of criteria evolved for the purpose, two particular sites located at Singara in the Nilgiris and Rammam in Darjeeling have been identified as the possible sites. Apart from these, another exciting possibility appears to be the 8800 meters long tunnel under Rohtang Pass near Manali. A summary and comparison of these possible sites is given below.

In the next section we outline the criteria which were used in site characterisation.

Site Requirements: In order to have some uniform criteria to prepare a report on possible sites for INO, the following criteria were suggested[1]:

The recommended evaluation criteria may include the following factors :

1. History of the site: Mainly availability of the site on a long term basis.

2. Cost factors: Construction costs, operating costs. Existing underground projects like hydro-electric plants are better since many of the facilities such as access roads and housing would already be present and save costs.

3. Risk Factors and Safety issues:

    - Rock conditions risk: This risk factor includes multiple considerations relative to the risk of capital and operating cost overruns due to unexpected rock conditions. Forecasting based on known stress conditions may help in anticipating such a risk.

[1]These criteria were gleaned from our own experience as well as by looking at similar studies in other locations, especially the documents related to the proposal for a National Underground Science Laboratory in the US[18]. We have benefitted much from these earlier or ongoing projects

- Environmental Risk: The time and expense required at various sites to determine what is safe and environmentally sound.
- Seismic Risk: Although engineering can control seismic risk, there is an additional cost involved in installing detectors in a seismically active region. In addition, there is a risk of a more intense than expected earthquake or an engineering or installation mistake that leads to failure in an earthquake of expected magnitude.
- Mechanical Systems Risk: Sites with heavy equipment, hoisting or other machinery have an operating cost risk due to the possibility of failure of significant mechanical systems.

4. Depth: Apart from a reasonable overburden in all directions, a complete 3D topo map of the region must be prepared for evaluating backgrounds. Rock density, suitability for low radioactivity experiments.

5. Neutrino Beam: Though this is still way into the future, distances to various neutrino factories and any particular advantage that may be there due to physics reasons is an important factor.

6. Time to Install First Detectors: Perhaps the most important factor for INO to be competitive. Already completed projects require much less time to create a cavern for the laboratory.

7. Accessibility: Scientists will visit the INO from various parts of the country and the world. Access to the laboratory by air/train/road throughout the year is an important factor.

   Ease of Personnel Access: The perceived ease of personnel access to the laboratory is important both as a substantive factor and as a quality-of-life factor. Ideally, the laboratory should be available 24 hours per day, seven days per week.

PUSHEP Site: This site located in South India, situated in the southern peninsular shield (in South India) which offers one of the best tunnelling medium for the creation of an underground facility (North 11.5° and East 76.6°). The INO site will be an extension of an upcoming underground Hydel project located about 6.5 kms from a town called Masinagudi (90 km south of Mysore) at the edge of the Mudumalai sanctuary near the border between Tamil Nadu, Karnataka and Kerala. It is called the Pykara Ultimate Stage Hydro Electric Project (PUSHEP) and is being executed by the Tamil Nadu Electricity Board (TNEB). The powerhouse is located in a cavern underground accessed by a 1.5 km long tunnel. Fig.4.1 gives a panoramic view of the PUSHEP site. The underground cavern is 20 meters wide, 39 meters high and 70 meters long similar to the requirement of INO for locating the iron calorimeter detector. The existence of a number of tunnels is important for future forecasting. The site is also conveniently located in seismic zone-2, which implies a minimum seismic activity zone in India. A panoramic view of the site is shown in Fig.4.2

RAMMAM site: The INO site near the Rammam hydel project is located in the Eastern Himalayas at Lat. $27°24'N$ Long. $88°05.5'E$ in the district of Darjeeling in the state of West Bengal. It is at an elevation of 1450m and is about 140 kms away from Bagdogra airport and the city of Siliguri. Bagdogra is connected by air to both Kolkata (1 hr flight time)

Figure 4.1: A View of PUSHEP location from Glenmorgan.

Figure 4.2: Panoramic view of the Mountain at PUSHEP. The laboratory cavern will be located directly under the peak (2207 meters).

and Delhi airports. Siliguri is connected by train to Kolkata (overnight journey) and to Delhi. It takes about 6 hours by car to reach Rammam from Bagdogra/Siliguri. There are three alternate routes. The scenic hill town of Darjeeling, the district headquarters is closer - about 70 kms away (2.5 hrs) and again connected by two alternate routes.

The Rammam hydel project presently has an installed capacity of 4×12.75 MW. It uses the water from the Rammam river and in its future extension plans will utilise the water from the other river Lodhama.

The proposed portals of the access INO tunnel and adit are located adjacent to the metalled road leading to the Powerhouse (about 4km south) of the hydel project. They are within the hydel project settlement and connected through a network of metalled/non-

metalled road. Figs.4 and 4.4 shows photographs of the area at the proposed portal location. Multiple locations and depths for the laboratory are possible. The area is in seismic zone 4.

Figure 4.3: INO tunnel portal location at Rammam Site.

Figure 4.4: Panoramic view of the Rammam river valley.

Hence extra precautions needs to be taken during the construction stage. But there are a number of long tunnels and large caverns already built in and around this area. So it does not seem to be an unsurmountable problem.

Rohtang Pass Site: Apart from INO at PUSHEP and Rammam, another exciting possibility appears to be the 8800 meters long tunnel near Rohtang Pass at Manali. Two important

reasons that make this site particularly exciting are that only a cavern/chamber needs to be excavated and that the overburden may be more than any other site that we have surveyed until now.

The tunnel will bore through the Pir Panjal range in the Himalayas from Kullu-Manali valley into Lahaul-Spiti valley. The south portal is at an elevation of 3050m and the north portal is at an elevation of 3080m. The maximum vertical overburden being 1900m about 6km from the south portal. Veering to the left from the south will achieve overburden well in excess of 2000m. There will be ventilation on both sides, fire hazard monitoring cells, traffic hazard cells and even pollution monitoring cells. The tunnel road will be 10m wide, 10m high in horse-shoe shape allowing two-lane traffic. The overburden exceeds 1000m from about 3.8km to 6.8km from the south portal.

As far as INO at Rohtang possibility is concerned, one major civil engineering task will be automatically achieved because the 8.8km long tunnel provides multiple locations where caverns may be excavated as has been done at LNGS in Gran Sasso but with much larger overburden than in any other underground laboratory in the world rivalling only the the underground facilities that existed at KGF. The photograph in Fig.4.5 shows a panoramic view of the area. The Border Roads Organisation(BRO) is likely to create a campus around

Figure 4.5: View of the Rohtang Pass from the highest point at 3980m. The winding approach road from Manali is visible.

the beginning of the tunnel near Manali to provide dedicated power supply, ventilation system, water supply and fire services on much larger scale than needed for INO laboratory alone. This fact alone gives a tremendous advantage for INO since many of the maintainance aspects are already built in. Furthermore, the construction of caverns and smaller tunnels may also be undertaken by the same organisations that are involved in the Rohtang tunnel project on a turnkey basis for INO.

While these factors make this proposal promising there are some issues, minor or major, that need further study:

- The project site is situated in Seismic Zone-4 after recent reclassification.
- The time scale of the proposed project is supposed to be between seven to nine years from the start.
- Access to the tunnel is from Manali or near about. There is a small airport at Kullu which is connected to Delhi by air. Nearest railhead on broad gauge is nearly 300km away. However, Manali is connected by road to Shimla, Chandigarh and New Delhi.
- There are several avalanche points along the access road to the south portal which need to be continuously managed. Further, the area near the portal will be snow bound with heavy snow in winter. While the agencies may clear snow to keep the tunnel operational, it is likely to create delays.

4.1 Tunnel and Cavern Complex

The description given below provides a feasible baseline access and laboratory designs that satisfies the scientific needs of INO. These may change depending on detailed geological mapping of the site and as the INO needs are fully developed. No finality in design is presumed.

Surface laboratory and Portal: Once the location of the portal is decided at a chosen site for INO, an important next step is the extent and availability of land for surface laboratories, if any.

Design of access tunnel: There are two feasible options for the design of tunnels. Single tunnel or two tunnel access. The main factors that will dictate the appropriate option will be cost and safety issues. While the single tunnel option is cost effective, the twin-tunnel is expensive but safer.

Cavern complex: The orientation of the cavern complex is tentatively fixed as running from North to South in PUSHEP extrapolating from the Geo technical data available at present. The exact location and orientation of the underground complex depends on the detailed data that will be obtained and monitored as the tunnel construction progresses in the chosen site.

A schematic view of the Cavern complex based on the present design of PUSHEP powerhouse complex is given in Fig. 4.6

4.2 Comparison of PUSHEP and Rammam

The atmospheric muon background flux at these two sites may be gleaned from Fig.4.7 where the depth is measured in MWE (depth times the density of matter). Corresponding depths of some well-known labs are indicated in the figure for comparison. Other features of INO at PUSHEP and Rammam are summarised in Tables 4.1 and 4.2.

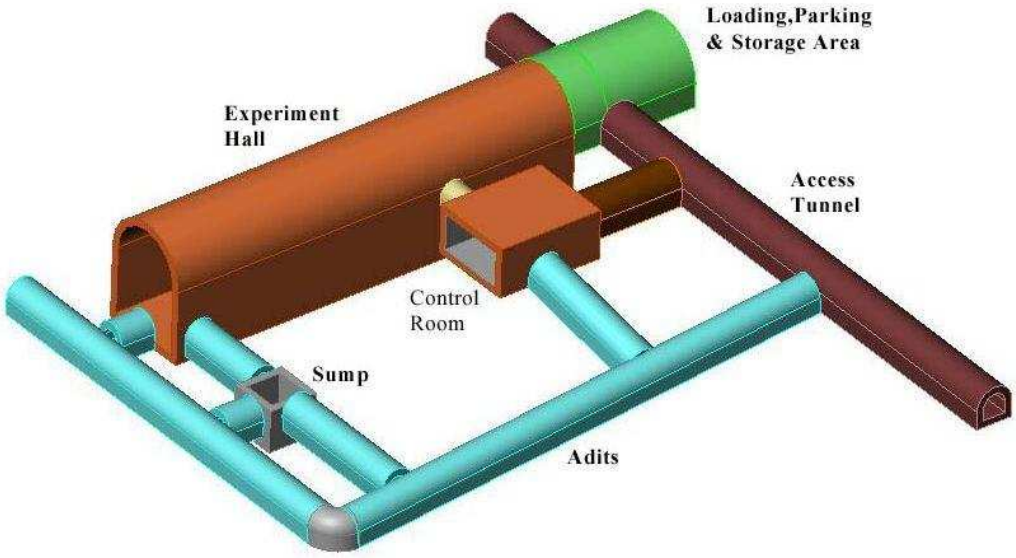

Figure 4.6: An artist illustration of the Laboratory Cavern Complex

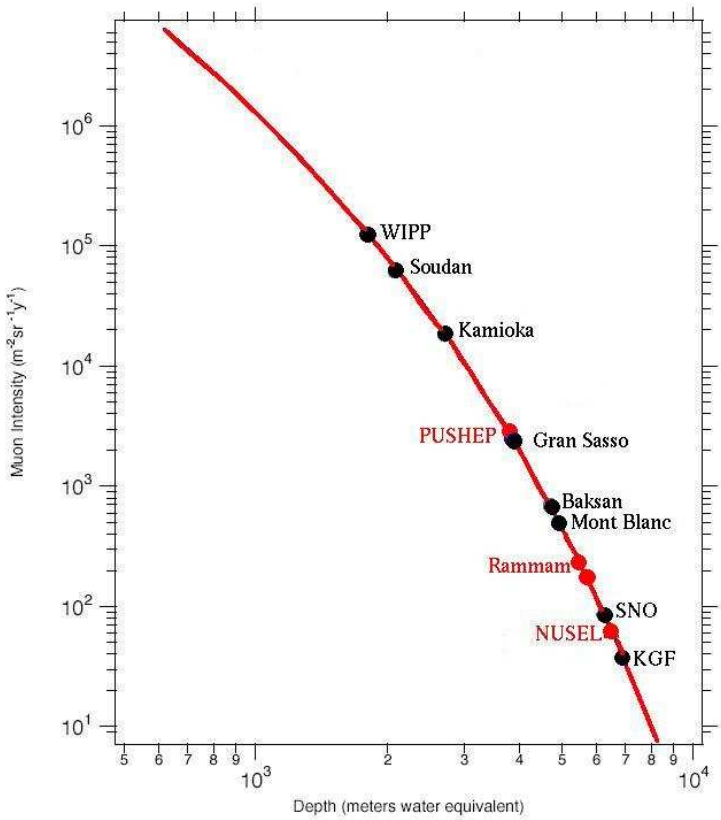

Figure 4.7: Atmospheric muon background as a function of depth. The Best locations for INO correspond to background as in Gran Sasso or better. The Rohtang site is not shown in the above, but the background may be comparable to KGF if not better.

Criteria	PUSHEP	Rammam
1. Site History:	Singara project since 1930s; PUSHEP built to last 100yrs	Operating since 1995
2. Transportation: Site access:	 Masinagudi(7km) Ooty(30km) Mysore (90 kms) Coimbatore (100 kms) Calicut (120 kms) Bangalore (250 kms)	 Lodhama(5km) Darjeeling(70km) Siliguri(140km)
Nearest Railhead:	Mysore (North) Coimbatore(South) Calicut (West)	N.Jalpaiguri (150km)
Nearest Airports:	Coimbatore(domestic) Calicut(domestic) Bangalore (Int'l)	Bagdogra(domestic) Kolkata(Int'l)
3. Geo technical Data: Rock Quality: Q-factor (tun. Medium): H/V stress ratio: (1-2 is desirable) Seepage: Geological Adversities Geological Mapping: Support Measures: Stand up time: Rock Radio-activity:	 Charnockite(Monolith) (Sg.2.62-2.9) 4-45: Good to V.Good Approximately 1.6 Moist to Dry. No known adversities Shears, dykes, joints mapped from both surface projections and underground tunnels PCC lining, Shotcreting, rock bolting. 3months to infinity 0.005mR/hr- Very low	 Gneiss (Sg.2.79-2.84) Fair to V.Good Not available Moist No known adversities Shears, joints mapped from surface studies Shotcreting, rock bolting 1-90 days Not available
4. Neutrino Beam baseline: CERN (Magic baseline) JHF Fermi Lab	 7100 km 6600 km 11300 km (with 3700 km of core)	 7100 km 5000 km 10600 km (no core)

Table 4.1: Comparison of various features at PUSHEP and Rammam.

Criteria	PUSHEP	Rammam
5.Laboratory Features:		
Lab Location	Below 2207m at ≈ 900 m	Below 2880m at≈ 850m
Lab Access:	Horizontal two way	Same
	Heavy eqp. transport	
Tunnel Option	Tunnel Length(km); Vertical Cover(m); All-round cover (m)	
Option-1	1.87; 1313; $\geq$ 1000	3.25; 1400; $\geq$ 1250
Option-2	2.13; 1299; $\geq$ 1000	3.85; 1680; $\geq$ 1500
Option-3	2.38; 1340; $\geq$ 1000	4.85; 1780; $\geq$ 1650
Gradient:	1:15 (reverse)	Horizontal
6.Risk Factors:		
Seismic Risk:	Zone-2	Zone-4
	No discernible faults	No faults
		on alignment
Environmental Risk:	Reserve Forest	Reserve Forest
	Portals inside	Portals inside
	TNEB/private land	WBSEB/Govt.Land
Civil Unrest/Terrorism:	None so far	None so far
7. Time Scale :		
Pre-Construction Stage:	$\leq$12 months	$\leq$ 12 months
Tunnel/cavern excavation		
with support measures:	About 22 months	About 41 months
Mechanical Outfitting:	12–18 months	12–18 months
8. Cost Saving Factors:		
Facilities:	Housing, GH	Housing, GH
	Access Road, Security	Access Rd, Security
	RAC/CRL,GH at Ooty.	
9. Academic Institutions:		
Educational	Bangalore, Mysore,	Siliguri, Darjeeling
Institutions:	Coimbatore, Calicut	
Research	Bangalore, Mysore, Coimbatore,	Darjeeling, Kolkata
Institutions:	Ooty (TIFR RAC/CRL)	
10.Environmental Factors:		
Weather:	Moderate(min.12-25°)	Moderate (Min. 5-20°C)
Rainfall/year:	Low (100-150cm)	Mod.Heavy(300-400cm)
Access:	24hrs/365 days	Almost all days
Biosphere:	Wildlife sanct.	Wildlife sanct.

Table 4.2: Comparison of various features at PUSHEP and Rammam–contd. The time factor for driving tunnels and cavern construction are based on L&T estimates and are to be regarded as approximate guide-lines.

Chapter 5

Strategies for Human Resource Development

INO will require a substantial investment in human resources. We have to train a large number of physicists and engineers who will ultimately be the backbone of INO and contribute to its success. Innovative ideas are needed in the recruitment and training of these physicists. Some of the INO members have already started giving lectures to students in Colleges, Universities and other institutions, exposing them to recent discoveries in neutrino physics and to the possibility of doing front-line neutrino experiments in India. While a lot of interest has been expressed by students on INO, we do not have a suitable mechanism as yet, to exploit this abundant resource available in the country. This will be one of the high-priority items before us.

Human Resources Needs The human resources needed for a large project like INO are varied: Broadly they are classified as:

- Construction and installation: Mainly Civil and mechanical engineers and scientists involved in the installation of the detector and data systems. While the civil and mechanical works will be entrusted to appropriate external agencies, INO will need its own engineers to ensure all design requirements are met.
- Maintainance and operations: After the installation of the detector, approximately about 15 engineers/scientists will be needed to ensure continuous running of the detector throughout the day.
- End user groups: This groups consists physicists- faculty/students/postdocs- who are members of the INO collaboration. A collaboration of this type needs at least 50 people including about 30 scientists. At any time about 15 members of this group will be present on site conducting experiments and data analysis. Apart from these, there must be opportunities for students and visiting scientists to pursue project at the site.

The required human resources, scientific, may be generated in about four to five years time, some strategies are outlined below.

INO Training School: One solution is to start a Training School, either separately or attached to one of the existing training programs at BARC, CAT, that can train about 15 MSc/B.Tech/BE students every year at an all-India level, so that in 5 years we would have

about 75 trained experimental physicists and some engineers. The trainees will be given jobs at one of the participating Institutions on the basis of successful performance in the Training School.

The trainees would be taught the relevant subjects like, high energy and nuclear physics, detector physics, computer simulation, data handling and analysis. There is enough expertise in the country to undertake such an endeavour. If desired, the scope of the Training School may also be expanded to include all of Experimental HEP projects including the Neutrino Project.

A Joint Universities Training Programme: Another possibility is to use the University system for this training programme. Many universities like Delhi University, Panjab University, Jammu University and University of Rajasthan already have an active experimental HEP programme. A joint universities training programme run by these HEP departments is yet another possibility.

Direct Recruitment Actually, best training could be imparted through hands-on experience in existing experiments on detector development activities, rather than class room teaching. On the basis of an all-India advertisement, about a dozen people could be recruited immediately. This can be repeated every year.Both physicists and engineers must be recruited.

Any one of these processes or a suitable combination of them must be initiated immediately.

Chapter 6

Cost and Time Schedules

We will provide some ball-park estimates of the cost and time scales for various tasks. No detailed estimates are available at present and the figures mentioned in this chapter are very preliminary estimates.

6.1 Cost Factors

The cost factors include the following items; details are listed in Table 6.1:

- Site: Each of the sites involves construction of tunnels, laboratory cavern and support structures. The actual cost depends on the nature of rock, availability of labour and ease of access[1].

  The approximate cost for the construction at PUSHEP is Rs. 30 crore, which includes an access tunnel (dia. 7m 'D' shaped) of length 2.2 kms and a cavern of dimensions 120 m $\times$ 20 m $\times$ 25 m (height).

  The corresponding figure for construction at Rammam is Rs. 80 crores, which includes a main access tunnel (dia. 7m 'D' shaped) of length 4.85 kms, an adit (dia. 7m 'D' shaped) of 2 kms and a cavern of the same dimensions as for PUSHEP.

  If the laboratory is located in Rohtang pass, there will a substantial saving since no access tunnel is required at this site.

- Civil Work: Some civil work will be needed at the point of access to tunnel portal, for structures to house the surface lab., and some buildings to house people who will work in the lab. The total cost of such civil work will be in the region of Rs. 35 crores; a break-up of the estimate is shown in Table 6.1. Furthermore, some facilities such as overhead-crane for lifting equipment and steel plates into place, air-circulation and air-conditioning in the lab and tunnel are required. This will cost roughly Rs 20 crore.

- Iron: A total of 35 ktons (or more) of iron rolled into plates is required for ICAL. Normal mild steel costs around Rs. 40 per kg[2] and has a saturation magnetic field of about 1–1.4 Tesla. The cost of iron is expected to be around 140 crores. Here we have

[1] The estimates given here are based on the budgetary estimates given by **L & T** Limited

[2] The figure in 2003 was Rs 20 per kg. A recent escalation of the costs has already driven this price up to about Rs.40 per kg.

No.	Item	Cost (Rs in crores)	
		PUSHEP	Rammam
I	LAB CONSTRUCTION (surface and underground)		
1.	Tunnel and Cavern excavation	30	80
2.	Civil Work underground and on surface	35	
	(i) for the tunnel road		
	(ii) in the cavern		
	(iii) at surface lab		
	(iv) for hostel buildings		
	(v) for flats/other accomodation		
3.	Facilities in the cavern	20	
	(i) overhead crane		
	(ii) air circulation in tunnel		
	(iii) air-conditioning the lab		
	(iv) electrical work		
	Total cost of lab construction	85	135
II	COST OF IRON		
4.	Iron (at Rs 40 per kg)	140	
	Total cost of iron	140	140
III	OTHER DETECTOR-RELATED COST		
5.	Magnetisation	15	
6.	Detector	80	
	(i) RPC		
	(ii) strip plates		
	(iii) front-end electronics		
	(iv) power supply		
	(v) gas circulation system		
7.	Electronics and DAQ	20	
8.	Contingencies	30	
	Total detector-related cost (excl iron)	145	145
	TOTAL	370	420

Table 6.1: Estimated total cost of INO underground laboratory and ICAL detector at INO at the two possible sites, PUSHEP and Rammam. Where only one column is filled, the cost is the same at both sites. Note that the cost of iron is substantial but it can be re-used.

not taken into account the fact that if any special modification in the composition of steel is required for magnetisation purposes this will increase the cost further.

It may be noted that there is no degradation of iron—once the experiment is finished, it can be reused. **Even though this is one of the biggest components of the total expenditure of INO, it is a recoverable expenditure.**

- Magnetisation: Approximately around 15 crores, including the cost of coils and machining.

- Detector: Approximately around 80 crores for the detector elements including glass plates, strip plates, front-end electronics, power supply, gas system.

- Electronics and Data acquisition: Approximately about 20 crores for DAQ, trigger, external veto, etc.

The total estimated cost of building the laboratory along with the ICAL detector is therefore expected to be around Rs. 370 crores in PUSHEP and about Rs. 420 crores in Rammam., of which Rs 140 crores (for the iron) is recoverable and Rs 30 crores has been added for contingencies. (The figures for the site at Rohtang will be similar to PUSHEP or even less depending on the local geological information.) The major cost goes into setting up the facilities at the surface as well as making the underground laboratory. Note that the underground laboratory will be a National facility and can be used for other types of experiments also.

The figures given above do not include the operating cost at either of these sites. This again is site dependent.

6.2 Time Scale

The project may be executed in three phases once the approval is given in principle:

- Phase 1 of approximately 12-18 months duration: Site investigation to draw up detailed design reports for tunnel and cavern complex. This could be faster if all the permissions are easily available and and the work entrusted to reputed engineering group/s.

  Detailed design reports on the detector structure, RPC, pick-up electrodes, front-end electronics, power supply systems.

- Phase 2: Tunnel and cavern excavation, support measures, etc. The estimated time at PUSHEP is 22 months. The estimated time at Rammam is 41 months[3].

  Basic design of RPC as already available will be frozen by this time. Tenders for the supply of iron, magnet coil, cables. Manufacture procedure for detector elements, electronics, gas mixing units and begin the production process.

- Phase 3 of approximately 12-18 months duration: laboratory outfitting, transport of detector components and material and assembly. The first module may be completed early, and start data taking. Ends with the laboratory occupancy and data taking by the second module.

[3]Based on L& T estimates

Chapter 7

INO as a facility for the future

In chapter 3 a discussion of the main physics problems that are envisaged to be undertaken at INO with ICAL was given. ICAL is only the first detector to be put in the INO laboratory. In the future, INO is expected to house other neutrino detectors, especially for low energy neutrino detection. Apart from neutrino physics and neutrino astronomy, an underground laboratory offers possibilities for studies on several important and current problems in physics and other fields. After the closure of the laboratory at KGF there has been no such underground laboratory in the country. We recall the main advantages of such a laboratory:

- Low cosmic ray background as exemplified by Fig.4.7. If the site has in addition low rock radioactivity, experiments requiring low background in high and low energy radiation can be undertaken.
- Reduction in the vibration levels due to surface activities.

We list some of the fields that can be profitably started and studied in such an underground laboratory:

- One of the interesting features that needs further study in connection with solar neutrinos is the day–night effect. A solar neutrino detector as close to the equator as possible is advantageous for such studies[36]. A heavy water detector is under consideration and the physics possibilities with such a detector are being analysed.
- Experiments involving neutrinos from nuclear reactors in the vicinity of such a laboratory, can yield information on neutrino properties.
- A long term watch for neutrinos from stellar collapse (supernovae) can be undertaken from such a laboratory.
- About 40% of the heat outflow from the earth is estimated to be generated from terrestrial radioactivity, mainly from the decay of U^{238} and Th^{232}. There are several models for the distribution of these materials in the earth. These can be tested by studying low energy neutrinos in an underground laboratory[37].
- Neutrino Tomography of the Earth may be undertaken by studying the matter effects on the phenomena of oscillation of neutrinos from laboratory produces and atmospheric neutrinos[38].

- Low background conditions like the ones obtainable in an underground laboratory with low rock radioactivity are required for studying important and rare processes like neutrino-less double decay. As already mentioned in the introduction, such experiments (a few of which are already under operation) give important information on the Dirac or Majorana nature of neutrino. A Majorana mass as low as 0.2 eV or lower may be determined from such an experiment.

- There is continuing interest in low energy(up to a few hundred KeV) nuclear cross sections that are relevant in nuclear astrophysics like the capture of α-particle on ^{12}C in stellar nucleosynthesis. A low energy high current accelerator in an underground laboratory (like LUNA in Gran-Sasso) with suitable low energy particle detectors can serve this purpose. Dark matter and dark energy searches is yet another possibility in any underground laboratory.

- The low background conditions may be utilised to study detector and material development.

- The reduction of vibration due to surface activity can be helpful in the study of Gravitational Waves.

- Seismic studies, subsurface studies in life-sciences, nuclear test monitoring, etc.

It is obvious that there is a need for a well equipped underground laboratory from several points of view. The realisation of the INO project can initiate such programmes in the country.

Bibliography

[1] The list of references on Standard Model and Neutrino oscillations is huge[1]. Here we give references to books and reviews where all the essential details needed for this report are available:
J.N. Bahcall, *Neutrino Astrophysics* (Cambridge Univ.Press, 1989);
G. Rajasekaran. *Phenomenology of neutrino oscillations*, *Pramana*, **55**, 19 (2000);
R. N. Mohapatra and Palash Pal, *Massive neutrinos in Physics and Astrophysics*(World Scientific, Singapore, 2004);
N.G. Cooper, Ed., *Celebrating the Neutrino*, Published in "Los Alamos Science", No. 25 (1997).
D. Indumathi, M.V.N. Murthy and G. Rajasekaran, Eds., *Perspectives in Neutrino Physics*, Proceedings of Indian National Science Academy **76** (2004).

[2] B. T. Cleveland, *et al. Astrophys. J.* **496**, 505 (1998); Nucl. Phys. B (Proc. Suppl.) **38**, 47 (1995); W. Hampel *et al.*, (The Gallex collaboration), *Phys. Lett.* **B447**, 127 (1999); J.N. Abdurashitov *et al.*, (The SAGE collaboration), *Phys. Rev.* **C60**, 055801 (1999); M. Altmann *et al.*, (The GNO collaboration), *Phys. Lett.* **B492**, 16 (2000); Y. Fukuda *et al.*, (The Super-Kamiokande collaboration), *Phys Rev. Lett.* **82**, 2430 (1999); **86** 5651 (2001); Q. R. Ahmad, *et al.*,(The SNO collaboration), *ibid.* **87**, 071301 (2001); B. Aharmim *et al.* (SNO Collaboration), hep-ex/0407029; M. B. Smy *et al.* (Super-Kamiokande Collaboration), *Phys. Rev.* **D 69** (2004) 011104, hep-ex/0309011; S. N. Ahmed *et al.* (SNO Collaboration), nucl-ex/0309004. J. Yoo *et al.* (Super-Kamiokande Collaboration), *Phys. Rev.* **D 68** (2003) 092002, hep-ex/0307070.

[3] Y. Fukuda, Y. *et al.*(Super-Kamiokande Collaboration), *Phys. Rev. Lett.***81** (1998) 1562-1567, hep-ex/9807003; Y. Fukuda, *et al.* (Super-Kamiokande Collaboration),*Phys. Rev. Lett.***82** (1999) 2644-2648, hep-ex/9812014; W.W.Allison, W. W. M. *et al.* (Soudan-2 Collaboration), *Phys. Lett.***B449** (1999) 137-144, hep-ex/9901024; Ambrosio, M. *et al.* (MACRO Collaboration), *Phys. Lett.***B478** (2000) 5-13; S. Fukuda, **et al**. (Super-Kamiokande Collaboration), *Phys. Rev. Lett.***85**(2000) 3999-4003, hep-ex/0009001; M. Ambrosio *et al.* (MACRO Collaboration), *Phys. Lett.***B566** (2003) 35, hep-ex/0304037; M. Sanchez *et al.* (Soudan 2 Collaboration),*Phys. Rev.* **D68** (2003) 113004, hep-ex/0307069;

[4] Figure taken from the talk presented by P. Bhattacharjee at the Neutrino-2001 meeting, The Institute of Mathematical Sciences, Chennai, February 2001.

[1] In order to keep this report concise, we have not given a complete list of references, but only a representative list to help the reader interested in further reading

[5] Neutrino mass limits have been reviewed recently by: Carlo Giunti, hep-ph/0308206. NuFact 03, 5th International Workshop on Neutrino Factories & Superbeams, 2003; Christian Weinheimer, hep-ex/0306057. 10th Int. Workshop on Neutrino Telescopes, Venice/Italy, March 2003; Jean-Luc Vuilleumier, hep-ex/0306010. XXXVIII Rencontres de Moriond, Electroweak interactions and Unified Theories, 2003.

[6] S. Goswami, talk at Neutrino 2004, see S. Goswami, A. Bandyopadhyay and S. Choubey, arXiv:hep-ph/0409224.

[7] M. C. Gonzalez-Garcia, hep-ph/0410030. Nobel Symposium on Neutrino Physics.

[8] K.S. Hirata, K. S. *et al.* (Kamiokande-II Collaboration), *Phys. Rev.***D38** (1988) 448.

[9] R. Cisneros, *Astro. Sp. Sci.* **10**, 87 (1971); M. Voloshin, M. Vysotskii, L.B. Okun, *JETP* **64**, 446 (1986), *Sov. J. Nucl. Phys.* **44**, 440 (1986); For a recent review see, Yifang Wang, hep-ex/0411028. Talk given at 32nd International Conference on High Energy Physics, 2004, Beijing, P.R. China.

[10] C. Athanassopoulos, *et al* LSND Collaboration, *Phys. Rev.Lett.* **81**, 1774 (1998); *Phys. Rev.* C**58**, 2489 (1998).

[11] Y. Ashie *et al.* (Super-Kamiokande Collaboration), hep-ex/0404034;

[12] G. Bhattacharyya, H.Pas, L. Song and T.J. Weilere, *Phys.Lett.***B564**, 175 (2003); hep-ph/0302191.

[13] The details of the MONOLITH proposal may be seen at http://castore.mib.infn.it/ monolith/

[14] For a comprehensive list of ongoing, future experiments as well as theory of neutrino oscillations, solar neutrinos and atmospheric neutrinos see The Neutrino Oscillation Industry Page at http://www.hep.anl.gov/ndk/hypertext/nuindustry.html and follow the links; another useful site for comprehensive information on the status of neutrino physics is The Ultimate Neutrino Page athttp://cupp.oulu.fi/neutrino/;

[15] Detection of muons produced by cosmic ray neutrinos underground, C.V. Achar et al., *Phys. Lett.* **18**, 196 (1965).

[16] The KGF Collab., M.R. Krishnaswamy, M.G.K. Menon, N.K.Mondal, V.S. Narasimham, B.V. Sreekantan, Y. Hayashi, N. Ito, S. Kawakami, S. Miyake, *Nuovo Cimento* **C 9** (1986) 167.

[17] M.R. Krishnaswamy *et al., Phys. Lett.* B **57**, 105 (1975); *Pramana*, **5**, 59 (1975).

[18] For details of the National Underground Science and Engineering Laboratory proposal see http://int.phys.washington.edu/NUSEL/

[19] Some details of the INO proposal may be seen at http://www.imsc.res.in/∼ino. The site is still under construction.

[20] M.Anelli et. al, Nucl. Inst. and Meth. A 300(1991) 572.

[21] Z. Maki, M. Nakazawa, S. Sakata, *Prog. Theor. Phys.* **28**, 870 (1962).

[22] M. Maltoni *et al.*, hep-ph/0405172.

[23] M. Apollonio *et al.* [CHOOZ Collaboration], *Phys. Lett.* B **466**, 415 (1999), hep-ex/9907037.

[24] V. Agrawal, T. K. Gaisser, P. Lipari and T. Stanev, Phys. Rev. D **53**, 1314 (1996) [arXiv:hep-ph/9509423].

[25] M. Honda, T. Kajita, K. Kasahara and S. Midorikawa, *Phys.Rev.* **D70**, 043008 (2004),astro-ph/0404457.

[26] For details see, D. Indumathi and M.V.N. Murthy, *A question of hierarchy: Matter effects with atmospheric neutrinos and anti-neutrinos*, hep-ph/0407336.

[27] A. Datta, R. Gandhi, P. Mehta and S. U. Sankar, *Atmospheric neutrinos as a probe of CPT and Lorentz violation*, *Phys.Lett.* B **597**, 356 (2004), hep-ph/0312027;

[28] V. D. Barger *et al.*, *Phys. Rev. Lett.* **85**, 5055 (2000) [arXiv:hep-ph/0005197].

[29] T.D.Lee and C.N.Yang, *Phys rev* **98** , 1501 (1955); L.B.Okun, *Sov J Nucl Phys*, **10** 206 (1969); For a review see A.D.Dolgov , *Phys Rep.* **320**, 1 (1999).

[30] A.S. Joshipura and S. Mohanty, *Constraining long-range leptonic forces using iron calorimeter detectors*, PRL Preprint, October 2004.

[31] C. Albright *et al.*, hep-ex/0008064; See also the web site http://gate.hep.anl.gov/ndk/hypertext/nufactory.html for a complete listing of proposals around the world.

[32] R. Gandhi, P. Ghoshal, S. Goswami, P. Mehta and S. U. Sankar, *Large matter effects in nu/mu → nu/tau oscillations*,hep-ph/0408361; R. Gandhi, P. Ghoshal, S. Goswami, P. Mehta and S. Uma Sankar, work in progress;

[33] R. Saakian, Nucl. Phys. Proc. Suppl. **111**, 169 (2002).

[34] I. S. Alekseev and G. T. Zatsepin, Proc. Intern. Conf. on Cosmic Rays, Moscow, Vol.1, p.324, 1960; R. P. Kokoulin and A. A. Petrukhin, NIM A263, 468, 1988; R. P. Kokoulin and A. A. Petrukhin, Sov. Journ. Part. Nucl. 21, 332, 1990.

[35] A. de Rujula *et al.,* Phys. Rev. Lett. **35**, 628 (1975); G. Rajasekaran and K.V.L. Sarma, *Pramana* **5**, 78 (1975); J.C. Pati and A. Salam, Preprint ICTP/75/73, (1975).

[36] Mohan Narayan, G. Rajasekaran and Rahul Sinha, *Modern Physics Letters* A **13**, 1915 (1998).

[37] There are several papers on geo-neutrinos; important among them are R.S. Raghavan *et al., Phys. Rev. Lett.* **80**, 635 (1998); H. Nunokawa *et al.,* hep-ph/0308175; F. Mantovani *et al.,* hep-ph/0309013. K. Eguchi *et al.,*(KamLAND) *Phys. Rev. Lett.* 90 (2003) 021802;S. Mohanty, hep-ph/0302060; R.S. Raghavan, hep-ex/0208038.

[38] The neutrino tomography of the earth was proposed in A. De Rujula, S. Glashow, R. Wilson and G. Charpak, *Phys. Rep.* **99**, 341 (1983).